AIMS Mathematics, 10(9): 21953–21993.
DOI: 10.3934/math.2025978
Received: 23 July 2025
Revised: 06 September 2025
Accepted: 15 September 2025
Published: 22 September 2025

https://www.aimspress.com/journal/Math

Survey

Variational formulation of a fully-three-dimensional non-linear beam dynamics by a Lie-group representation

Simone Fiori*

Dipartimento di Ingegneria dell'Informazione, Università Politecnica delle Marche, Via Brecce Bianche, I-60131, Ancona, Italy

* **Correspondence:** Email: s.fiori@staff.univpm.it.

Abstract: This paper presents a survey of a geometrically exact beam theory formulated within the framework of Lie groups, aimed at providing a mathematically consistent description of slender structures undergoing large displacements and rotations. The beam configuration is modeled as a curve in the space $\mathbb{SO}(3) \times \mathbb{R}^3$, enabling a coordinate-free expression of the governing equations. A variational formulation serves as the basis for deriving the equations of motion, which emerge as nonstandard Euler-Lagrange equations on the configuration space. Strain measures arising from the group structure define the internal forces and moments, which couple to the dynamics via balance laws. The formulation automatically incorporates conservation of energy, linear momentum, and angular momentum, and reveals the underlying geometric structure through the appearance of Lie brackets in the angular momentum equation. This framework emphasizes the connection between geometry and mechanics, offering advantages in both physical fidelity and computational stability.

Keywords: geometrically exact flexible beam theory; inextensible Euler-Bernoulli beam; Reissner-Simo beam theory; Timoshenko-Ehrenfest beam; variational formulation
Mathematics Subject Classification: 70G45, 70G75

1. Introduction

Leonardo da Vinci appears to have been the first to attempt a formulation of beam theory, followed by Galileo Galilei about a century later. Leonardo da Vinci is credited with the key observation that, when a beam bends, some parts stretch and elongate, while others compress and shorten. This implies the existence of a point in each cross-section that remains unchanged during bending [57], leading naturally to the concept of the beam's "neutral line". Both scientists were held back by the lack of two fundamental theoretical tools, namely, Robert Hooke's elasticity theory and differential calculus developed by Isaac Newton and Gottfried Wilhelm Leibniz.

The first consistent formulation of a beam theory is attributed to Leonard Euler and Daniel Bernoulli, who built on the work of Jacob Bernoulli and published what is now known as *Euler-Bernoulli beam theory*. Remarkably, Euler-Bernoulli theory was made use of extensively in the design, and ultimately allowed the building, of the Eiffel Tower in Paris. Euler-Bernoulli theory was built off a number of hypotheses that make the results obtainable by its application inaccurate in the case, for example, of stubby beams. More specialized theories have also emerged, such as the Cosserat rod theory [37], which generalizes the Kirchhoff–Love rod model. The latter describes one-dimensional slender rods while accounting only for bending and twisting deformations [34].

The first remarkable advancement after the Euler-Bernoulli theory was due to Stephen Timoshenko and Paul Ehrenfest and is now known as *Timoshenko-Ehrenfest beam theory* [14, 34]. A comparison of the main beam theories from the scientific literature is presented in Table 1.

Table 1. Breakdown of the main beam theories from the scientific literature.

Theory	Main assumptions	Deformation modes	Rotational effects	References
Euler-Bernoulli	Cross-sections remain normal to neutral axis; shear deformation is neglected	Bending only	No rotational inertia	[66]
Timoshenko-Ehrenfest	Accounts for shear deformation; cross-sections do not necessarily remain perpendicular	Bending and shear	Includes rotational inertia	[66]
Cosserat (Micropolar)	Cross-sections can deform and rotate independently (micro-rotations)	Bending, shear, torsion, axial	Includes independent rotational degrees of freedom	[3, 12]
Levinson	Higher-order shear deformation theory; parabolic shear strain distribution	Bending and shear (higher-order accuracy)	Enhanced accuracy without shear correction factors	[44]
3D Nonlinear Beam (Antman)	Full 3D kinematics; large displacements and rotations; includes geometric and material nonlinearities	Bending, shear, torsion, axial	Fully nonlinear with all rotational effects	[3, 56]

Beam theory provides a basis for predicting the behavior of, e.g., cantilever beams subjected to mechanical loads [35, 55, 64] and also to study DNA chain dynamics [16], to analyze the mechanical behavior of solar panels and antennas [58], to design compliant mechanisms [69] and bio-inspired sensing structures [70], and to design astronautical applications [47] and locomotion systems [6].

An application of flexible beam theory of particular interest is related to soft manipulators [65].

The main factors driving research in the design, modeling, and control of continuum manipulators are reachability, high dexterity, and significant elastic deformability, as the constituents of soft manipulators are capable of bending, torsion, shear, elongation, and large deformations. Magnetic actuation in soft robotics offers advantages over other actuation mechanisms, including high dexterity, versatility, and possibility of wireless control. By applying remote magnetic torques to permanent magnets or coils embedded within the manipulator's body or at its tip, the motion and configuration of the manipulator can be controlled. Dynamic models of manipulators are crucial for control, trajectory planning, and optimal design, particularly in minimally invasive surgery sessions.

A modern mathematical model of elastic beams is known as the *geometrically exact Simo-Reissner beam*, which builds on a minimal number of assumptions on the kind of deformations that a beam is subjected to when loaded [51, 63]. The geometrically exact beam theory is a nonlinear theory used to describe the motion and deformation of slender structures (beams) capable of accounting for large displacements, rotations, and strains. It is often used in aerospace, civil, and mechanical engineering applications where beams experience complex deformations. A key feature of this theory is that it accounts for arbitrarily large displacements and rotations, expressed by rotation matrices or quaternions. In Simo-Reissner's beam theory, strains are typically small, but rotations can be large. The equations of motion may be derived using the Lagrange-d'Alembert principle or Newton-Euler equations and involve forces and torques, which are typically expressed in a body-fixed coordinate system.

Geometrically exact beam theory accounts for general three-dimensional beam deformations such as spatial bending, torsion, axial tension, and shear deformation. The accounting of shear effects makes the geometrically exact beam theory adequate to describe thick rod dynamics. It has been referred to as 'geometrically exact' because it is consistent regardless of the magnitude of displacements, rotations, and strains [34]. A geometrically exact beam model includes a number of relevant phenomena, as detailed below:

- *Shear stress* – A kind of deformation that denotes the component of stress coplanar with a material cross section, which arises from the shear force, the component of force parallel to the material cross section.
- *Normal stress* – A further type of deformation that arises from the force component perpendicular to the material cross section on which it acts.
- *Deflection* – Deformation of the beam that arises when a part of a beam is deformed laterally (namely, in a direction transverse to its longitudinal axis) under a load.

In a geometrically exact beam model, there is no restriction on the normal of a cross section to be parallel to the tangent to the line of centroids.

Geometrically exact beam theory found application in the study of rotor blades, robotic arms, flexible structures, and aerospace-class components (see, e.g., [10, 55, 58, 64, 67]). It can be coupled with finite element methods (FEM) for computational modeling. Compared with classical beam theories, it can capture shear, bending, torsion, and axial deformations more accurately. Unlike Euler-Bernoulli or Timoshenko-Ehrenfest beam theories, geometrically exact beam theory does not make small-angle or small-displacement assumptions.

The purpose of this survey is to present a formal recount of the geometrically-exact beam theory by the language of Lie-group theory as an instrument to describe exactly the motion of a flexible beam

undergoing large deformations. The starting point is the partitioning of a beam into independent rigid sections and the construction of a Lagrangian function that accounts for the kinetic energy of each section, an elastic energy that couples sections to one another, and the potential energy that couples the section to the external environment (most notably, to a gravitational and to a magnetic field). As a general theoretical tool to get the equations of motion, the Lagrange-d'Alembert principle is invoked and paired to the variational method. This extended principle enables the inclusion of effects that are not directly derived from a Lagrangian formulation, including external loads and frictional forces.

Starting from the general, non-linear mathematical model, a number of simplified models are studied as arising from appropriate assumptions. Notably, deriving the inextensible non-linear Euler-Bernoulli beam theory deviates from one such logical flow as it involves differential constraints whose implementation requires re-running the calculus of variation by either the method of 'distribution' or the method of Lagrange multipliers, which are shown to be equivalent to one another.

Outline of the paper–Section 2 recalls a mathematical model of a flexible beam based on Simo-Reissner geometrically exact beam theory formulated in a variational fashion. In particular, the potential energy in the Lagrangian of a beam includes explicitly a magnetic energy term to include magnetic-type control in the general model. Section 3 outlines a number of theoretical features of the recalled mathematical model, such as energy/momenta conservation. Section 4 describes the relationship between the general model and a number of simpler instances, including a full inextensible Euler-Bernoulli theory. Section 5 concludes this survey.

2. Geometrically exact mathematical model of a flexible beam

In order to obtain a mathematical model of a flexible beam, we shall invoke the Lagrange-d'Alembert variational formulation based on the notion of Lagrangian function. The Lagrangian density (per unit of length) of a flexible beam takes the expression [15, Section 2.2]

$$L := K - E - U, \tag{2.1}$$

where K denotes the kinetic energy density of the beam per unit of length, E denotes the elastic potential energy density of the beam per unit of length, and U denotes a potential energy density per unit of length that the beam couples with. In a Lagrange-d'Alembert formulation, further theoretical elements need to be considered, as detailed in the following sections. For an alternative Hamiltonian formulation, interested readers might consult [16].

Equation (2.1) introduces the Lagrangian L as a combination of three energy contributions, namely the kinetic energy K, the elastic (strain) energy E, and the potential energy of external forces U. This formulation encapsulates the beam's full dynamical behavior in a variational framework. The kinetic energy K accounts for the inertial effects associated with both translational and rotational motion of the beam's cross-sections. The elastic energy E measures the internal deformation cost, arising from stretching, bending, and shearing – encoded through geometrically exact strain measures. The potential energy U, on the other hand, represents the work done by external fields (such as gravity) acting on the beam. The principle of stationary action then dictates that the evolution of the system minimizes the action integral of L, yielding the equations of motion that naturally balance inertia, elasticity, and external forcing. This compact formulation is especially effective for modeling beams undergoing large displacements and rotations.

A geometrically exact beam model consists of a chain of cross-sections, each of which is a rigid body that may translate and rotate relative to each other to accommodate for stretching, bending, and twisting which causes shear across sections. As each section may move spatially, it possesses a kinetic energy. Elastic energy bonds sections together, and the potential energy describes, albeit partially, what makes the sections move besides the internal forces. External loads and non-conservative solicitations complete the model under the form of distributed forces and torques.

2.1. Reference frames and general definitions

In the present endeavor, we shall assume that a beam may be decomposed into infinitely many, infinitely thin, cross-sections indexed by a continuously varying parameter $x \in [0,\ \ell]$, with $\ell > 0$. Each cross-section is characterized by a thickness $\mathrm{d}x$ and is assumed to be isotropic and homogeneous, hence it is characterized by a frontal surface $\mathcal{A}(x)$ and a mass density function $\varrho(x)$. We shall also adopt Bernoulli's hypothesis, according to which, no cross section is subjected to any change in thickness and surface area during its motion. Each cross-section may undergo translation and rotation relative to adjacent sections as a result of the beam's deformation.

It is important to underline that we shall establish the equations of motion with respect to two sets of reference frames: *An inertial reference frame and a moving reference frame fixed to each cross-section*. The deformed state of a beam may be described by two functions [62, Section 1 & 2.1], namely $\phi : [0,\ \ell] \times [0,\ T] \to \mathbb{R}^3$, which represents the configuration of the line of centroids of the beam (or simply 'centerline'), and $R : [0,\ \ell] \times [0,\ T] \to \mathbb{SO}(3)$, which represents the instantaneous orientation of each section relative to an inertial reference frame, as outlined in Figure 1. The constant $\ell > 0$ may be interpreted as the length of the centerline in an undeformed (rest) configuration, while the constant time $T > 0$ denotes the duration of an observation.

Deformed configuration: $(\phi(x,t), R(x,t))$ Undeformed configuration: $(\phi_0(x), I_3)$

Figure 1. Example of undeformed (rest) configuration and a deformed configuration of a flexible beam (dashed line: line of centroids).

A formal property that is emphasized in the specialized literature is termed 'frame indifference' (or material indifference or frame independence). This is a property of any quantity whose value remains invariant upon the transformation

$$\begin{cases} \phi \to Q\phi + c, \\ R \to QR, \end{cases} \tag{2.2}$$

for every $c \in \mathbb{R}^3$ and every $Q \in \mathbb{SO}(3)$. A frame-indifferent function of the pair (ϕ, R) takes the same value independently of the reference frame in which it is evaluated.

2.2. Kinetic energy of a flexible beam

Given a cross-section x and a material point within, of coordinate $\xi \in \mathbb{R}^3$ with respect to the material reference system attached to this cross-section, its position at time t in the inertial frame is expressed as $\phi(x,t) + R(x,t)\xi \in \mathbb{R}^3$.

The velocity of motion of a material particle is given by $\partial_t(\phi(x,t) + R(x,t)\xi)$, hence the kinetic energy density per unit length of the beam at section x and time t is evaluated as

$$K(x,t) := \frac{1}{2}\int_{\mathcal{A}(x)} \|\partial_t\phi(x,t) + \partial_t R(x,t)\xi\|^2 \,\varrho(x)\,\mathrm{d}A(x). \tag{2.3}$$

The physical interpretation of this expression requires an understanding of the velocity field of material points within each cross-section. Each material point within the cross-section x has a position ξ relative to the cross-section's local coordinate system. The absolute velocity of this material point in the inertial reference frame is given by $v(\xi,x,t) = \partial_t\phi(x,t) + \partial_t R(x,t)\xi$. This velocity field consists of two distinct physical contributions: $\partial_t\phi(x,t)$, which denotes the translational velocity of the cross-section's centroid and represents the motion of the beam's centerline through space, and $\partial_t R(x,t)\xi$, which denotes the velocity induced by the rotation of the cross-section about its centroid, which imparts additional velocity to the material points located away from the centroid. The kinetic energy calculation follows the formula for distributed systems. For each infinitesimal material element with a mass density $\varrho(x)$ and an area element $\mathrm{d}A(x)$, the contribution of kinetic energy is $\frac{1}{2}\varrho(x)\|v(\xi,x,t)\|^2\,\mathrm{d}A(x)$. The total kinetic energy density of the entire cross-section is obtained by integrating over the cross-sectional area $A(x)$. This formulation captures the fundamental physics that the beam's kinetic energy arises from two sources: The translation of each cross-section through space and the rotation of each cross-section, which generates additional kinetic energy for points distributed away from the centroid. The squared Euclidean norm $\|\cdot\|^2$ ensures that all three spatial velocity components contribute to the kinetic energy, while the area integration accounts for the distributed nature of the beam's mass. The approach treats each cross-section as a rigid body capable of translation and rotation, which is essential to the geometrically exact beam theory's ability to accurately model large deformations while preserving the kinematic assumption that cross-sections remain undeformed during motion.

The kinetic energy (2.3) may be broken down into three terms, namely the translational energy of each material point on the centerline, the rotational energy of each section, and a cross-term

$$K = \frac{1}{2}\|\partial_t\phi\|^2\left(\int_{\mathcal{A}}\mathrm{d}A\right)\varrho + \frac{1}{2}\mathrm{tr}\left(\partial_t R\left(\int_{\mathcal{A}}\xi\xi^\top\mathrm{d}A\right)\partial_t R^\top\right)\varrho + \partial_t\phi^\top\partial_t R\left(\int_{\mathcal{A}}\xi\,\mathrm{d}A\right)\varrho \tag{2.4}$$

where the superscript $^\top$ denotes transposition and the operator $\mathrm{tr}(\star)$ denotes matrix trace. (In references like [41, 62], the Euclidean inner product $\mathrm{tr}(N^\top B)$ of two matrices N, B is denoted as $N{:}B$.) For convenience of notation, let us set

$$\varrho_0(x) := \varrho(x)\int_{\mathcal{A}(x)}\mathrm{d}A,\ J(x) := \varrho(x)\int_{\mathcal{A}(x)}\xi\xi^\top\mathrm{d}A, \tag{2.5}$$

where the function ϱ_0 represents a mass density function per unit of length and is sometimes referred to as 'running mass', while $J(x)$ denotes a (non-standard) material surface rotational inertia tensor.

Recalling that the rotational velocity may be expressed in terms of the material angular velocity $\Omega(x,t) \in \mathfrak{so}(3)$ (also referred to as 'vorticity' in the specialized literature) by $\partial_t R(x,t) = R(x,t)\Omega(x,t)$, and that, by the very definition of 'line of centroids', it follows that

$$\int_{\mathcal{A}(x)} \xi \, \mathrm{d}A \equiv 0, \ \forall x \in [0, \ \ell]. \tag{2.6}$$

The kinetic energy density of a beam may be recast as

$$K(x,t) = \tfrac{1}{2}\|\partial_t \phi(x,t)\|^2 \varrho_0(x) + \tfrac{1}{2}\mathrm{tr}(\Omega^\top(x,t) J(x) \Omega(x,t)). \tag{2.7}$$

The mass density function could be spatially variable so as to account for incidental or designed inhomogeneity in the material (due, for instance, to inserts of magnetic materials). In any case, it is straightforward to prove that the above-defined kinetic energy function enjoys the property of frame indifference.

The Euler-Bernoulli beam theory disregards the rotational component of the kinetic energy, while the geometrically-exact beam theory incorporates such a contribution as a non-negligible one.

2.3. Elastic energy

Starting from an undeformed state, provoking a deformation of a beam requires energy in the form of mechanical work. Such energy is stored within the material and may later be released as the undeformed shape is restored. It is assumed that an undeformed state is characterized by a straight centerline and by untwisted cross-sections.

The elastic energy density quantifies the amount of energy stored within the beam per unit of length and is commonly expressed as [15, Section 2.2]

$$E(x,t) := \tfrac{1}{2}(\epsilon(x,t) - \mathrm{e_x})^\top C(x)(\epsilon(x,t) - \mathrm{e_x}) + \tfrac{1}{2}\mathrm{tr}(\Gamma^\top(x,t) D(x) \Gamma(x,t)) \tag{2.8}$$

where $\epsilon : [0, \ \ell] \times [0, \ T] \to \mathbb{R}^3$ denotes material strain (quantifying the extension and shearing of the beam's axis), $\Gamma : [0, \ \ell] \times [0, \ T] \to \mathfrak{so}(3)$ denotes material torsion (and measures its curvature), and C, D denote 3×3 diagonal stiffness matrices for axial/shear and bending/torsion deformations, respectively. The stiffness matrix D, in particular, is a nonstandard one. The stiffness may certainly vary across the beam, although it is a common practice to approximate it to be constant. The material strain (or translational strain) and torsion (or rotational strain, also referred to as material curvature) are defined as [15, Section 2.2]

$$\epsilon := R^\top \partial_x \phi, \ \Gamma := R^\top \partial_x R, \tag{2.9}$$

respectively, while $\mathrm{e_x} \in \mathbb{R}^3$ denotes the (tangent) unit vector associated with the undeformed centerline – assumed to be straight.

Equation (2.8) expresses the elastic energy density stored per unit length of the beam due to deformation from its natural (undeformed) state. This energy density captures the fundamental physics of elastic deformation through two distinct mechanisms: Stretching/shearing and bending/twisting. The first quadratic term in definition (2.8), namely the expression $\frac{1}{2}(\epsilon(x,t) - \mathrm{e_x})^\top C(x)(\epsilon(x,t) - \mathrm{e_x})$, represents the *extensional and shearing energy*. Here, $\epsilon(x,t) = R^\top \partial_x \phi$ measures the material strain, which quantifies how much the beam's centerline deviates from its

natural configuration. The difference $\epsilon - \mathrm{e_x}$ represents the departure from the unstretched, unsheared state, where $\mathrm{e_x}$ corresponds to the tangent vector of the undeformed centerline. The stiffness matrix $C(x)$ relates strain to the internal forces required to maintain that deformation, with larger eigenvalues of $C(x)$ indicating greater resistance to stretching or shearing in specific directions. The second quadratic term, namely $\frac{1}{2}\mathrm{tr}(\Gamma^\top(x,t)D(x)\Gamma(x,t))$, captures the *bending and torsional energy*. The material curvature $\Gamma(x,t) = R^\top \partial_x R$ measures how rapidly the cross-section orientation changes along the beam's length. This quantity encodes both bending (curvature in the beam's plane) and twisting (rotation about the beam's longitudinal axis). The stiffness matrix $D(x)$ relates these curvature measures to the internal moments required to sustain the deformation. Both energy contributions follow the principle that elastic energy is proportional to the square of the deformation measures, consistent with Hooke's law for small strains extended to finite rotations. The trace operator in the second term ensures that all components of the curvature tensor contribute to the stored energy. The stiffness matrices $C(x)$ and $D(x)$ encode the material properties (such as Young's modulus and shear modulus) as well as the geometric properties of the cross-section (much like area and second moments of area). This formulation naturally satisfies frame indifference: The stored energy depends only on the relative deformation between neighboring cross-sections, not on the beam's overall position or orientation in space. The energy density integrates over the beam's length to yield the total elastic potential energy, which drives the beam's motion through the variational principle.

We refer to $\epsilon(x,t)$ as material strain in the present survey, as in [13, Section 2.3] and [19, Section 3]. Other sources use different conventions, for example, in [15, Section 2.2], it is referred to as 'convected velocity', while, e.g., in [36, Section 2.3], the translational strain is defined as $R^\top \partial_x \phi - \mathrm{e_x}$. If the undeformed state of the material is more nontrivial than a straight centerline and untwisted cross-sections, it is necessary to introduce two reference functions $\epsilon_0(x)$ (which takes values in $\mathbb{R}^3$) and $\Gamma_0(x)$ (which instead takes values in the algebra $\mathfrak{so}(3)$) and to modify the expression of the elastic energy as

$$\begin{aligned} E(x,t) := {} & \tfrac{1}{2}(\epsilon(x,t) - \epsilon_0(x))^\top C(x)(\epsilon(x,t) - \epsilon_0(x)) \\ & + \tfrac{1}{2}\mathrm{tr}((\Gamma(x,t) - \Gamma_0(x))^\top D(x)(\Gamma(x,t) - \Gamma_0(x))). \end{aligned}$$

Geometrically exact beam theories are well-suited for modeling beams with initial geometric imperfections, like curvature or twist. For example, a recent finite-volume formulation based on the Simo-Reissner geometrically exact beam [7] explicitly supports arbitrary initial curvatures and has been demonstrated to converge accurately under large displacement regimes. Additionally, advanced finite element variants, including both Kirchhoff-Love and Simo-Reissner types, have been rigorously evaluated for slender beams undergoing 3D dynamics with arbitrary initial curvature and anisotropic sections [51], preserving objectivity and delivering strong numerical performance. These studies show that geometric imperfections do not fundamentally invalidate geometrically exact theory. Rather, these studies highlight the need for formulation choices that maintain kinematic consistency and numerical robustness in curved or defected beam configurations.

The first quadratic term on the right-hand side may be referred to as *potential extensional and shearing energy*, while the second term may be referred to as *potential bending and torsion energy* [40, Section 2.1]. If necessary, the bending strain stiffness and the torsional strain's stiffness may be regarded as time-dependent parameters. The above-defined elastic energy density is treated as a potential energy in the Lagrangian as it stays stored until it gets released. The expression above for the elastic energy meets the requirement of frame indifference, [19, Section 3] and [13, Section 2.3].

2.4. Magneto-gravitational potential energy function

The beam is assumed to exist within a field accounting for a number of effects, much like gravitational and magnetic contributions [65, Section 4.3]. These specific effects may be accounted for by introducing a potential energy density per unit of length of the form

$$U(x,t) := g\,\mathrm{e}_z^{\top}\phi(x,t)\,\varrho_0(x) - b^{\top}(\phi(x,t),t)R(x,t)\,m(x)\,\varrho_0(x) \tag{2.10}$$

where g denotes the *local* gravitational acceleration (assumed to be constant), $\mathrm{e}_z \in \mathbb{R}^3$ denotes the vertical unit vector – directed upward – so that the product $\mathrm{e}_z^{\top}\phi$ denotes the altitude of the x-centroid, $b : \mathbb{R}^3 \times [0,\ T] \to \mathbb{R}^3$ denotes a possibly time-varying magnetic induction field acting on the beam and $m : [0,\ \ell] \to \mathbb{R}^3$ denotes the specific magnetic dipole moment per unit of mass of the x-section of the beam (so, that, in fact, the product $m\,\varrho_0$ represents a magnetic dipole moment density per unit of length).

In the relations above, it was implicitly assumed that the dipole moment of a cross-section is time-invariant, although it will not be difficult to account for a time-dependent one. It is perhaps necessary to underline that the potential energy function, in general, depends on time, and therefore it does *not* give rise to a conservative force field. We shall underline that, while the kinetic and elastic energy terms are frame-indifferent, the potential energy terms need not be.

2.5. Variational principle

In order to determine the equations of motion of each cross-section of a beam, we shall proceed by means of the Lagrange-d'Alembert principle. It consists of considering two continuously varying families of curves, namely

$$\phi = \phi(x,t;s),\ R = R(x,t;s), \tag{2.11}$$

indexed by a parameter $s \in [-a,\ a]$, with $a > 0$, where the index value $s = 0$ conventionally refers to the actual (or fiducial) motion state of the beam.

The invoked variational principle, in the present context, may be expressed as

$$\int_0^T \int_0^\ell \delta L(x,t)\,\mathrm{d}x\,\mathrm{d}t + \int_0^T \int_0^\ell (f^{\top}(x,t)\delta\phi(x,t) + \mathrm{tr}(\Theta^{\top}(x,t)\,\delta R(x,t)))\,\mathrm{d}x\,\mathrm{d}t = 0 \tag{2.12}$$

where the variation symbol δ denotes the passage from the actual trajectory to an infinitesimally close trajectory as the index s varies infinitesimally, which boils down to the application of the operator $\partial_s|_{s=0}$. The first term on the left-hand side represents the variation of the action, while the second term represents the virtual work of the external force field $f : [0,\ \ell]\times[0,\ T] \to \mathbb{R}^3$ and of the external torque field $\Theta : [0,\ \ell]\times[0,\ T] \to \mathfrak{so}(3)$. The symbols $\delta\phi : [0,\ \ell]\times[0,\ T] \to \mathbb{R}^3$ and $\delta R : [0,\ \ell]\times[0,\ T] \to \mathfrak{so}(3)$ denote variations associated with the curves $(x,t) \mapsto \phi(x,t)$ and $(x,t) \mapsto R(x,t)$, which are induced by the passage to infinitesimally close paired curves in the space $\mathbb{R}^3 \times \mathbb{SO}(3)$, to be defined shortly. (As a reference, readers might like to consult the review paper [13] and, in particular, Section 3.6 therein. As a general reference on the action principle, we shall mention the scientific report [11] that offers a novel geometrical and physical interpretation.)

The external force and torque may be present in a model because they represent external loads on a beam (see, for instance, the example discussed in [15, Section 4.2]) or the interaction with a

fluid [48, 60], as well as control actions, which are of interest in soft manipulator design [65], in active control of vibration [1], and in the control of prosthetic or wearable devices [52]. Since loads as well as control actions may be distributed along the beam (even though they may act at discrete points), technically the force field f is a force density per unit of length; likewise, the mechanical torque field Θ is a torque density per unit of length. A fundamental aspect of the invoked variational principle is that boundary/temporal conditions enter directly into the calculations.

The complete Lagrangian density function reads as follows:

$$\begin{aligned} L = {} & \tfrac{1}{2}\varrho_0 \|\partial_t \phi\|^2 + \tfrac{1}{2}\mathrm{tr}(\Omega^\top J \Omega) - \tfrac{1}{2}(\epsilon - \mathrm{e_x})^\top C(\epsilon - \mathrm{e_x}) \\ & - \tfrac{1}{2}\mathrm{tr}(\Gamma^\top D \Gamma) - g\varrho_0\, \mathrm{e_z}^\top \phi + \varrho_0\, b^\top R\, m. \end{aligned} \tag{2.13}$$

Table 2 shows the units of each variable introduced so far. Incidentally, due to unit equivalences, unrelated quantities turn out to exhibit identical units. It is not hard to verify that both terms on the left-hand side of the relation (2.12) exhibit the correct unit of action, J·s.

Table 2. Detail of the measurement units (expressed in the International Unit System, where J = Joule, m = meter, kg = kilogram, s = second, Wb = Weber, — = unitless).

Quantity	SI Unit
C, K, E, U, L, Θ	J/m
ξ, x, ϕ	m
A	m^2
ϱ	$\mathrm{kg/m}^3$
$\mathrm{e_x}$, $\mathrm{e_y}$, $\mathrm{e_z}$, ϵ, R	—
ϱ_0	kg/m
Γ	1/m
Ω	rad/sec
D	J·m
g	$\mathrm{m/s}^2$
b	$\mathrm{Wb/m}^2$
m	$\mathrm{J{\cdot}m}^2/\mathrm{kg{\cdot}Wb}$
f	$\mathrm{J/m}^2$
J	kg·m

The variational approach presented here has been further developed to accommodate more complex scenarios, including systems with embedded discontinuities for failure modeling [67] and gradient-based optimization applications [50]. The latter development is particularly relevant for automated design processes, as the Lie group structure naturally supports automatic differentiation techniques, enabling efficient computation of design sensitivities without the numerical complications that arise in coordinate-based formulations.

2.6. Mechanical stresses and momenta density along the beam

In order to facilitate the writing of some equations and quantities, we shall introduce the operator $\sigma : \mathbb{R}^{3\times 3} \to \mathfrak{so}(3)$, which we shall define as

$$\sigma(X) := \tfrac{1}{2}(X - X^\top) \tag{2.14}$$

which extracts the skew-symmetric component from a square matrix.

The stress density per unit of length along the beam (adapted from [15, Section 2.2]) is defined as

$$n := -\frac{\partial L}{\partial \epsilon} = C(\epsilon - \mathrm{e_x}) \tag{2.15}$$

and accounts for shear and stretch stresses. The relationship above, of the form $n = n(\epsilon)$, is essentially Euler's classical linear stress-strain constitutive equation, which was generalized in several ways, as in the Voigt model, used to account for viscoelasticity effects [45, Section 1].

The internal momentum density along the beam (adapted from [15, Section 2.2]) is defined as

$$M := -\frac{\partial L}{\partial \Gamma} = \sigma(D\Gamma) \tag{2.16}$$

and accounts for bending and torsional momenta. The two expressions above represent the so-called *constitutive relations* of the material.

The generalized translational momentum density per unit of length of each cross-section is likewise defined as

$$q := \frac{\partial L}{\partial\, \partial_t \phi} = \varrho_0\, \partial_t \phi, \tag{2.17}$$

while the generalized angular momentum density reads as

$$\Pi := \frac{\partial L}{\partial\, \Omega} = \sigma(J\Omega). \tag{2.18}$$

As a matter of fact, the Lagrangian density might be rewritten in terms of those new variables as

$$L = \tfrac{1}{2}\partial_t \phi^\top q + \tfrac{1}{2}\mathrm{tr}(\Omega^\top \Pi) - \tfrac{1}{2}(\epsilon - \mathrm{e_x})^\top n - \tfrac{1}{2}\mathrm{tr}(\Gamma^\top M) - g\varrho_0\, \mathrm{e_z}^\top \phi + \varrho_0\, b^\top R\, m. \tag{2.19}$$

This is indeed a far more general expression that accommodates more general constitutive relations of the material (see, for example, the note on Wagner strain in [49, Section 2.5] and [33, Section 2]). Besides, the following quantity

$$\frac{\mathrm{d}}{\mathrm{d}t}\int_0^\ell \left(\tfrac{1}{2}(\epsilon - \mathrm{e_x})^\top n + \tfrac{1}{2}\mathrm{tr}(\Gamma^\top M)\right) \mathrm{d}x \tag{2.20}$$

is what, in [62, Section 2.2], is referred to as 'stress power'.

We have mentioned in Section 2.2 and in Section 2.3 that the inertia tensor J and the stiffness tensor D are *not standard* (some authors refer to these tensors as 'dual'). Non-standard inertia tensors differ from standard ones–generally tabulated in the literature–although they are related to one another by a simple relation (for a review on this subject, see, e.g., [22, Section 2.2]). In particular, using J_s and D_s to denote the standard versions of those tensors, their non-standard version are calculated as

$$J = \tfrac{1}{2}\mathrm{tr}(J_\mathrm{s})I_3 - J_\mathrm{s},\ D = \tfrac{1}{2}\mathrm{tr}(D_\mathrm{s})I_3 - D_\mathrm{s}, \tag{2.21}$$

where I_3 denotes the 3×3 identity matrix. The standard version of these tensors should be positive-definite in order for the energy densities to be well-defined.

2.7. Detailed calculations

In the present section, we shall compute explicitly the variations of the three components of the action for an elastic beam, namely the kinetic component, the elastic component and the potential component. One might certainly proceed instead from a more general ground as in [41] and then derive the same equations by plugging in the Lagrangian function (2.13).

In order to recast the relation (2.12) explicitly, it pays to define the following independent variations:

$$\delta\phi(x,t) := \frac{\partial\phi}{\partial s}(x,t;0) \in \mathbb{R}^3,\ \delta R(x,t) := R^\top(x,t;0)\frac{\partial R}{\partial s}(x,t;0) \in \mathfrak{so}(3), \tag{2.22}$$

which represent the infinitesimal changes that occur to the centerline's shape and to the cross-section's orientation when passing from the actual configuration to an infinitesimally close further configuration.

Variation of the kinetic component of the action functional. In order to evaluate the variation of the kinetic component of the action, it is necessary to evaluate the derivative of the kinetic energy density (2.7) with respect to the index s at $s = 0$. This derivative reads as follows

$$\partial_s K|_{s=0} = (\partial_t\phi)^\top(\partial_s\partial_t\phi|_{s=0})\varrho_0 + \mathrm{tr}(\Omega^\top J\partial_s\Omega|_{s=0}). \tag{2.23}$$

The application $(x,t,s) \mapsto \phi(x,t,s)$ is assumed to be sufficiently regular such that $\partial_s\partial_t\phi = \partial_t\partial_s\phi$ for any $(x,t,s) \in [0,\ \ell] \times [0,\ T] \times [-a,\ a]$. In addition, from the very definition of an angular velocity matrix, it is readily found that

$$\partial_s\Omega = \Omega\,\delta R - \delta R\,\Omega + \partial_t\delta R, \tag{2.24}$$

under the assumption that the application $(x,t,s) \mapsto R(x,t,s)$ is sufficiently regular for the Schwarz-Clairaut property $\partial_s\partial_t R = \partial_t\partial_s R$ to hold on the parallelepiped $[0,\ \ell] \times [0,\ T] \times [-a,\ a]$. Notice that

$$\mathrm{tr}(\Omega^\top J(\Omega\,\delta R - \delta R\,\Omega)) = \mathrm{tr}(\Omega^2 J\delta R), \tag{2.25}$$

since Ω is skew-symmetric and the matrix product $\Omega^\top J\,\Omega$ is symmetric. As a result, the variation of the kinetic component of the action along the actual configuration takes the form

$$\begin{aligned}\int_0^T\int_0^\ell \partial_s K|_{s=0}\,\mathrm{d}x\,\mathrm{d}t = &\int_0^T\int_0^\ell (\varrho_0\,\partial_t\phi)^\top(\partial_t\delta\phi)\,\mathrm{d}x\,\mathrm{d}t\\ &+\int_0^T\int_0^\ell \mathrm{tr}(\Omega^2 J\delta R)\,\mathrm{d}x\,\mathrm{d}t\\ &+\int_0^T\int_0^\ell \mathrm{tr}(\Omega^\top J\partial_t\delta R)\,\mathrm{d}x\,\mathrm{d}t.\end{aligned} \tag{2.26}$$

The next step consists of expressing the first and the third integral on the right-hand side in terms of the variations $\delta\phi$ and δR only, which may be done by applying integration by parts, assuming that the Fubini-Tonelli theorem for exchanging integrals [24] applies. This operation leads to

$$\begin{aligned}\int_0^T\int_0^\ell \partial_s K|_{s=0}\,\mathrm{d}x\,\mathrm{d}t = &-\int_0^\ell\int_0^T (\varrho_0\,\partial_{tt}\phi)^\top\delta\phi\,\mathrm{d}t\,\mathrm{d}x\\ &+\int_0^\ell\int_0^T \mathrm{tr}(\sigma(\Omega^2 J)\,\delta R)\,\mathrm{d}t\,\mathrm{d}x\\ &+\int_0^\ell\int_0^T \mathrm{tr}(\sigma(\partial_t\Omega\,J)\,\delta R)\,\mathrm{d}t\,\mathrm{d}x,\end{aligned} \tag{2.27}$$

under the proviso that the following initial and final conditions are imposed:

$$\begin{aligned} &\partial_t\phi^\top(x,0)\,\delta\phi(x,0) = \partial_t\phi^\top(x,T)\,\delta\phi(x,T) = 0,\ \forall x\in[0,\ \ell],\\ &\mathrm{tr}(\Omega(x,0)J(x)\,\delta R(x,0)) = \mathrm{tr}(\Omega(x,T)J(x)\delta R(x,T)) = 0,\ \forall x\in[0,\ \ell]. \end{aligned} \tag{2.28}$$

If the beam assumes a fixed configuration at the beginning of the observation, the initial conditions are certainly verified as $\delta\phi(x,0) = 0$ and $\delta R(x,0) = 0$. If the final configuration is also fixed, then the final conditions are verified as well. On several occasions, however, only the initial conditions on $\phi(x,0)$, $\partial_t\phi(x,0)$ (the initial translational velocity), $R(x,0)$ and $\Omega(x,0)$ (the initial rotational velocity) are fixed (see, for instance, the example discussed in [15, Section 4.2]). In this case, if a solution to the equations of motion exists and is unique, then the final configurations $\phi(x,T)$ and $R(x,T)$ are determined uniquely by the initial conditions, and therefore $\delta\phi(x,T) = 0$ and $\delta R(x,T) = 0$ [45, Section 2]. Grouping terms according to the dependence from the variation of each independent variable leads to the expression

$$\delta\int_0^T\int_0^\ell K\,\mathrm{d}x\,\mathrm{d}t = -\int_0^\ell\int_0^T(\varrho_0\,\partial_{tt}\phi)^\top\delta\phi\,\mathrm{d}t\,\mathrm{d}x + \int_0^\ell\int_0^T\mathrm{tr}(\sigma(\partial_t\Omega+\Omega^2)\,J)\,\delta R)\,\mathrm{d}t\,\mathrm{d}x. \tag{2.29}$$

Variation of the potential energy component of the action functional. In order to evaluate the variation of the component of the action related to the external potential energy, it is necessary to evaluate the derivative of the potential energy density (2.10) with respect to the index s at $s = 0$. This derivative assumes the form

$$\partial_s U|_{s=0} = g\,\varrho_0\,\mathrm{e_z}^\top(\partial_s\phi|_{s=0}) - \varrho_0(\partial_\phi b|_{s=0}\partial_s\phi|_{s=0})^\top R\,m - \varrho_0\,b^\top(\partial_s R|_{s=0})m, \tag{2.30}$$

where the Jacobian matrix $\partial_\phi b$ represents the variability of the magnetic field across the beam. Since it holds that $\partial_s\phi|_{s=0} = \delta\phi$ and $\partial_s R|_{s=0} = R\,\delta R$, the expression above leads to

$$\partial_s U|_{s=0} = g\,\varrho_0\,\mathrm{e_z}^\top\delta\phi - (\varrho_0\,\partial_\phi b\,\delta\phi)^\top R\,m - \varrho_0\,b^\top R\,\delta R\,m. \tag{2.31}$$

Consequently, the variation of the component of the action related to the external potential may be written as

$$\delta\int_0^T\int_0^\ell U\,\mathrm{d}x\,\mathrm{d}t = \int_0^\ell\int_0^T\varrho_0\,(g\,\mathrm{e_z} - \partial_\phi^\top bR\,m)^\top\delta\phi\,\mathrm{d}t\,\mathrm{d}x - \int_0^\ell\int_0^T\mathrm{tr}(\varrho_0\,\sigma(mb^\top R)\,\delta R)\,\mathrm{d}t\,\mathrm{d}x, \tag{2.32}$$

by an application of a property of the matrix trace operator in the last integral on the right-hand side.

Variation of the elastic energy component of the action functional. To complete the calculations, it will be necessary to determine the variation of the component of the action related to the elastic potential energy by computing the derivative of the elastic energy density (2.8) with respect to the index s at $s = 0$. Start by observing that

$$\partial_s E|_{s=0} = (\epsilon - \mathrm{e_x})^\top C\,\partial_s\epsilon|_{s=0} + \mathrm{tr}(\Gamma^\top D\,\partial_s\Gamma|_{s=0}). \tag{2.33}$$

The application $(x,t,s)\mapsto\phi(x,t,s)$ is assumed to be sufficiently regular such that $\partial_s\partial_x\phi = \partial_x\partial_s\phi$ for any $(x,t,s)\in[0,\ \ell]\times[0,\ T]\times[-a,\ a]$. Likewise, the application $(x,t,s)\mapsto R(x,t,s)$ is taken to be sufficiently regular for the property $\partial_s\partial_x R = \partial_x\partial_s R$ to hold. Therefore, the variation of the strain and twisting read

$$\begin{cases}\partial_s\epsilon|_{s=0} = -\delta R\,\epsilon\ + R^\top\partial_x\delta\phi,\\ \partial_s\Gamma|_{s=0} = \Gamma\,\delta R - \delta R\,\Gamma + \partial_x\delta R,\end{cases} \tag{2.34}$$

which then yield the following expression for the variation of the elastic energy density:

$$\partial_s E|_{s=0} = (\epsilon - \mathrm{e_x})^\top C R^\top \partial_x \delta\phi + \mathrm{tr}(\sigma(\Gamma^2 D - \epsilon(\epsilon - \mathrm{e_x})^\top C)\delta R) - \mathrm{tr}(\sigma(\Gamma D)\partial_x \delta R). \tag{2.35}$$

While the second term on the right-hand side contributes directly to the equations of motion of a beam, the first and third term need to be reworked by applying integration by parts (with respect to the spatial variable x) under suitable boundary conditions. In detail, we may get

$$\int_0^T \int_0^\ell (\epsilon - \mathrm{e_x})^\top C R^\top \partial_x \delta\phi \,\mathrm{d}x\,\mathrm{d}t = -\int_0^T \int_0^\ell \partial_x((\epsilon - \mathrm{e_x})^\top C R^\top)\,\delta\phi \,\mathrm{d}x\,\mathrm{d}t \tag{2.36}$$

under the proviso that

$$\forall t \in [0,\ T],\ 0 = (\epsilon(x,t) - \mathrm{e_x})^\top C(x) R^\top(x,t)\,\delta\phi(x,t)|_{x=0}^{x=\ell}, \tag{2.37}$$

which holds, e.g., whenever the initial and final ends of a beam are kept fixed (clamped ends), in which case, $\delta\phi(0,t) = \delta\phi(\ell,t) = 0$ for all $t \in [0,\ T]$, or when [15, Section 2.3]

$$\epsilon(0,t) = \epsilon(\ell,t) = \mathrm{e_x},\ \forall t \in [0,\ T], \tag{2.38}$$

whose interpretation is that the centerline always stays orthogonal to the cross-sections at the ends of the beam. By the same token, we may get

$$\int_0^T \int_0^\ell \mathrm{tr}(\sigma(\Gamma D)\partial_x \delta R)\,\mathrm{d}x\,\mathrm{d}t = -\int_0^T \int_0^\ell \mathrm{tr}(\partial_x \sigma(\Gamma D)\,\delta R)\,\mathrm{d}x\,\mathrm{d}t \tag{2.39}$$

under the proviso that

$$\forall t \in [0,\ T],\ 0 = \mathrm{tr}(\sigma(\Gamma(x,t)D(x)\delta R(x,t)))|_{x=0}^{x=\ell} \tag{2.40}$$

which again holds in the case of clamped ends or when [15, Section 2.3]

$$\Gamma(0,t) = \Gamma(\ell,t) = 0,\ \forall t \in [0,\ T], \tag{2.41}$$

whose interpretation is that there is always no bending nor torsion at the end boundaries of the flexible beam. In conclusion, the variation of the elastic energy may be expressed as

$$\begin{aligned} \delta \int_0^T \int_0^\ell E\,\mathrm{d}x\,\mathrm{d}t = &-\int_0^\ell \int_0^T \partial_x((\epsilon - \mathrm{e_x})^\top C R^\top)\,\delta\phi\,\mathrm{d}t\,\mathrm{d}x \\ &+ \int_0^\ell \int_0^T \mathrm{tr}(\sigma(\Gamma^2 D - \epsilon(\epsilon - \mathrm{e_x})^\top C + \partial_x(\Gamma D))\,\delta R)\,\mathrm{d}t\,\mathrm{d}x, \end{aligned} \tag{2.42}$$

which may be used to derive the equations of motion of a flexible beam.

Summary of boundary conditions. In the previous calculations, the boundary terms were gotten rid of by imposing restrictions such as clamped ends. A summary of the boundary conditions often encountered in beam mechanics is given in Table 3. In several applications, mixed or traction/moment boundary conditions are needed, as the modeling of flexible beams often requires non-zero boundary conditions to accurately reflect physical constraints, actuation, or control inputs. For instance, in the context of boundary control and stabilization, non-zero boundary forces or moments are essential to

actively influence the beam's dynamics. The authors of [59] developed a boundary feedback control strategy for a geometrically exact beam model, where actuation at one end imposes a controlled non-zero boundary input, which is crucial for achieving exponential stabilization. Similarly, the authors of [2] analyzed the nonlinear vibrations of beams under various boundary setups, showing that clamped or pre-compressed boundaries significantly affect the vibrational modes and energy transfer, particularly near the instability thresholds. These applications illustrate that prescribed (non-zero) boundary conditions are not only mathematically admissible within geometrically exact frameworks, but also practically necessary in a wide range of problems related to control and structural dynamics. General boundary conditions may be expressed as $R\,n = \bar{t}$ and $M = \bar{M}$ at $x = 0$ and $x = \ell$, where $\bar{t} \in \mathbb{R}^3$ and $\bar{M} \in \mathfrak{so}(3)$ denote the applied end forces and momenta. As will be shown in Section 3.4, these forces and momenta give rise to power inputs to the beam-system.

Table 3. Summary of boundary conditions encountered in the variational formulation of flexible beam dynamics.

Type	Physical meaning	Mathematical expression
Clamped (Dirichlet)	Fixed position and orientation at endpoints	$\delta\phi(0,t) = \delta\phi(\ell,t) = 0$ $\delta R(0,t) = \delta R(\ell,t) = 0$
Free (Natural)	No internal force or moment applied at endpoints	$n(0,t) = n(\ell,t) = 0$ $M(0,t) = M(\ell,t) = 0$
Mixed	One end clamped and one free, or other combinations	e.g., $\delta\phi(0,t) = 0$, $n(\ell,t) = 0$
Temporal	Fixed variations at initial and final times	$\delta\phi(x,0) = \delta\phi(x,T) = 0$

2.8. Equations of motion of an elastic beam

Since the variations $\delta\phi$ and δR are arbitrary except on the boundary of the rectangle $[0,\ \ell] \times [0,\ T]$, from the variations above one deduces immediately the equations of motion of the centerline and of the rotations of the cross-sections as

$$\begin{cases} \partial_t R = R\,\Omega, \\ \varrho_0\,\partial_{tt}\phi - \partial_x(R\,C\,(\epsilon - \mathrm{e_x})) + g\,\varrho_0\,\mathrm{e_z} - \varrho_0\,\partial_\phi^\top b\,R\,m = f, \\ \sigma(J\,\partial_t\Omega) - \sigma(J\,\Omega^2) - \partial_x\sigma(D\,\Gamma) + \sigma(D\,\Gamma^2) - \sigma(C\,(\epsilon - \mathrm{e_x})\,\epsilon^\top) - \varrho_0\,\sigma(m\,b^\top R) = \Theta. \end{cases} \tag{2.43}$$

The equations of motion appear as coupled partial differential equations in the unknowns $\phi = \phi(x,t)$ and $R = R(x,t)$ in the independent spatial variable x and in the independent temporal variable t. It is important to break down the equations and provide a suitable interpretation of each term. In the present context, we have the following:

- *Second equation* – The term $\partial_{tt}\phi$ denotes the acceleration of the line of centroids, the term $\partial_x(RC(\epsilon - \mathrm{e_x}))$ denotes the internal cohesion force due to elasticity that tends to prevent a beam from elongating or getting compressed along its centerline, and the term $f - g\varrho_0\mathrm{e_z} + \varrho_0\,\partial_\phi^\top b\,R\,m$

denotes the resultant of the external forces acting on each section of the beam. We also point out that, since $\epsilon = R^\top \partial_x \phi$, the first equation is indeed second-order in both the temporal and spatial variables. It pays to notice that the distributed magnetic force $\varrho_0\, \partial_\phi^\top b\, R\, m$ takes a more familiar form if the specific magnetic dipole and the running mass are independent of the position on the centerline, in which case, it may be expressed as $\mathrm{grad}_\phi[(R\, m\, \varrho_0) \cdot b]$ in vector-calculus notation.

- *Third equation* – The term $\partial_t \Omega$ denotes the angular acceleration of each cross-section, while the quantity $\varrho_0 \sigma(J \partial_t \Omega) - \varrho_0 \sigma(J\Omega^2)$ represents Euler's torque for a rigid body, applied here to each cross-section of the beam. The term $\sigma(C(\epsilon - \mathrm{e_x})\epsilon^\top)$ denotes the bending torque on each section due to elasticity, whereas the term $\partial_x \sigma(D\Gamma) - \sigma(D\Gamma^2)$ denotes the restoring torque due to the stiffness of the material that tends to prevent a beam from twisting along its centerline. In addition, the term $\Theta + \varrho_0\, \sigma(m\, b^\top R)$ denotes the total torque exerted by the magnetic field and other external actions. Since $\Gamma = R^\top \partial_x R$, the second equation is also second-order in both independent variables. The term $\varrho_0\, \sigma(m\, b^\top R)$ may be represented as an axial vector proportional to the cross product $(R\, m) \times b$, which resembles the expression of the magnetic torque in vector-calculus notation.

Through meticulous work to identify and unify the notation, the system (2.43) was found to be fully compatible with the system (2.6a)+(2.6b) in [62], with the system (14) in [15], with the system (59) in [19] (which is written in mixed spatial/material frames), and with the system (4) in [65]. As a side note, we underline that we could introduce the axial operator $\mathrm{ax} : \mathfrak{so}(3) \to \mathbb{R}^3$ as $\mathrm{ax}[\sigma(uv^\top)] := \frac{1}{2} u \times v$. By this operator, one could easily interpret terms like $\sigma(n\epsilon^\top)$ as vector cross products. This is, in fact, the approach used by Eugster and Harsch in [19].

2.9. Model verification and limitations

Geometrically exact models based on centerline rotation have been directly validated against experimental data in the context of highly nonlinear cantilever dynamics. In a landmark study, Farokhi et al. conducted *in vacuo* base excitation experiments at two different acceleration levels ($\frac{1}{5}g$ and $\frac{1}{2}g$) to drive a cantilever into extremely large oscillations. High-speed imaging and image-processing techniques were used to extract tip displacements and rotations, which were then compared against the predictions of the geometrically exact model. The agreement was excellent across both moderate and extreme excitation levels, demonstrating the model's robustness and fidelity in capturing the nonlinear hardening behavior and complex motion of the beam [20].

Further experimental studies reinforce the accuracy of geometrically nonlinear beam models. For instance, González-Cruz et al. presented an experimental validation of a cantilever beam undergoing large geometric deformations, showing that its nonlinear dynamic response (especially under forced vibration) can be accurately captured by a simplified large-deformation model using a Galerkin-based approach. Their results confirmed the presence of characteristic nonlinear frequencies and highlighted the dominant role of structural damping in the dynamic behavior of these kinds of beams [28].

Additionally, Yoo et al. conducted experiments focusing on relatively large-amplitude oscillations of cantilevers, validating the applicability of the absolute nodal coordinate formulation in analyzing the nonlinear dynamics of beams [71]. Though not based on geometrically exact theory, these results lend support to geometrically consistent formulations by demonstrating accurate predictions of large deflections and dynamic behavior in beam systems.

While geometrically exact beam formulations excel at capturing large-deformation kinematics and dynamic nonlinearities, their reliability has limits when additional complexities enter the problem. In

fact, its validity can be compromised in contexts involving significant material nonlinearity beyond elastic limits, fracture or crack propagation, and numerical pathologies related to discretization and rotation representation. In these cases, coupling with models for plasticity, damage, and fracture mechanics or employing enriched numerical techniques becomes necessary to preserve predictive fidelity.

When the material's behavior deviates from purely elastic responses, such as plastic yielding, damage evolution, or other inelastic phenomena, the geometrically exact assumptions may become inadequate. The theory typically relies on constitutive laws grounded in elasticity, making its predictive capacity questionable when material nonlinearity dominates (e.g., yielding or plastic deformation, [27]).

Classical geometrically exact beam theory cannot by itself model fracture initiation or propagation. Fractures involve discontinuities and energy dissipation at crack tips or across failure surfaces, which are phenomena beyond the scope of continuous elastic formulations. Recent computational developments have attempted to bridge this gap. For example, Kota et al. [39] introduced a discontinuous Galerkin method combined with a cohesive zone model to describe fracturing in slender beams while retaining a geometrically exact beam description of the intact regions. Their approach demonstrates that modeling fractures requires additional interface mechanics beyond the standard beam theory.

Numerical discretization issues can also hinder robustness. As noted in the literature, challenges like singularities in rotation parametrization, shear locking, or non-convergent numerical schemes arise when modeling highly flexible, curved, or composite beams without careful formulation. These issues can compromise both accuracy and computational stability, particularly in complex geometries or under extreme loads.

3. Theoretical considerations

With the present section, we aim to present a number of considerations related to the geometrically exact beam model derived in the previous section, with the goal of enlightening its fundamental properties and at placing it within the context of beam theory.

3.1. Coordinate-free representation

Most contributions in the literature on beam theory present the equations of motion, as well as their derivation, through a coordinate-based notation. This amounts to choosing a 'convenient' way to represent the position of each cross-section (usually with three spatial coordinates, a function of time and a further spatial coordinate) and the orientation in space of each cross-section (most often via three angular coordinates such as Euler's angle), as well as their temporal and spatial derivatives. One such way of proceeding entails a large number of variables to manage, often related by lengthy trigonometric expressions. It is important to underline that the exact meaning of 'convenient representation' really depends on what aspect each author wishes to underline and what is exactly the purpose of a specific model [26, 32, 54].

As opposed to a coordinate-based approach, the present tutorial paper is written in the compact representation offered by Lie-group theory, where all the relevant variables are of vector type or matrix type and all mechanical forces and torques are expressed by the means of operators on vectors and

matrices. These operators are powerful yet fairly simple, such as matrix commutators, matrix/vector-to-matrix/vector products and the skew-symmetrization operator.

While a coordinate-based representation is certainly extremely useful in didactic contexts and to explore the behavior of flexible structure in details, a coordinate-free representation is more compact, appears more easy to implement by a high-level programming language for simulation purposes, and appears more convenient from a control-theoretic point of view. In particular, in the latter context, a matrix-based representation appears to be very convenient for designing and analyzing control methods (see, for example, the papers [21, 23] that illustrate this advantage in other applied scenarios).

The Lie group formulation offers several fundamental mathematical advantages beyond notational convenience. First, the representation automatically preserves essential geometric constraints: Rotations remain proper orthogonal matrices in $\mathbb{SO}(3)$ throughout the motion, eliminating the possibility of spurious numerical drift that might invalidate Euler angle representations [31, 38]. This intrinsic constraint satisfaction is particularly valuable in long-time simulations where accumulated errors in coordinate-based approaches can lead to non-physical configurations, such as reflection matrices or unnormalized rotation vectors.

The coordinate-free nature of the Lie group approach eliminates the singularities that commonly arise in local parameterization. Euler angles, for instance, suffer under gimbal lock configurations where degrees of freedom are lost, while quaternion representations require normalization constraints. The matrix Lie group $\mathbb{SO}(3)$ avoids these issues entirely, providing a global, singularity-free description of rotations that remains valid for arbitrarily large angular displacements [42, 46]. This property is essential for applications involving complete rotations or complex three-dimensional motions.

Recent advances in structure-preserving numerical integration have demonstrated significant advantages when applied to Lie group formulations of beam dynamics [8, 29]. The equations of motion can be integrated using methods that respect the underlying manifold structure, such as Lie group variational integrators, which exactly preserve discrete analogues of energy and momentum. These geometric integrators maintain the symplectic structure of Hamiltonian systems and prevent the artificial energy dissipation or growth that can occur with standard integration methods applied to coordinate-based formulations. The matrix-vector operations inherent in the Lie group approach align naturally with modern computational linear algebra libraries, enabling efficient implementation and automatic differentiation for sensitivity analysis or optimization. The clear separation between kinematics (encoded in the group structure) and dynamics (expressed through the Lagrangian) facilitates modular code design and systematic extension to more complex multibody systems or coupled field problems.

3.2. Equations of motions in terms of generalized variables

The equations of motion (2.43) may be rewritten in terms of generalized variables as

$$\begin{cases} q = \varrho_0\, \partial_t \phi,\ \Pi = \sigma(J\Omega),\ n = C(\epsilon - \mathrm{e}_x),\ M = \sigma(D\Gamma), \\ \partial_t q = \partial_x(R\, n) - g\varrho_0\, \mathrm{e}_z + \varrho_0\, \partial_\phi^\top b\, R\, m + f, \\ \partial_t \Pi + [\Omega, \Pi] = \partial_x M + [\Gamma, M] + \sigma(n\epsilon^\top) + \varrho_0\, \sigma(m\, b^\top R) + \Theta, \\ \partial_t R = R\, \Omega, \end{cases} \tag{3.1}$$

where $[A, B] := AB - BA$ denotes the matrix commutator. It is worth recalling that the equation of translation of the line of centroids is expressed in the inertial reference frame, while the equation of rotational dynamics about each section is expressed in the body-fixed reference frame attached to that section.

As a further note about the benefit of expressing the equations of motion in terms of generalized variables, we briefly mention that the natural configuration space of a geometrically exact beam is the Lie group SE(3), with the configuration field $g(x, t) \in \mathrm{SE}(3)$, the strains given by the Maurer-Cartan form [61] $g^{-1}\partial_x g \in \mathfrak{se}(3)$, and the velocities $g^{-1}\partial_t g \in \mathfrak{se}(3)$. Here, the curved space SE(3) denotes the special Euclidean group, while the linear space $\mathfrak{se}(3)$ denotes its Lie algebra. This formulation preserves frame indifference in a direct way, since rigid body motions act by group multiplication, and ensures the material objectivity of the strain measures. The current formulation uses the split description $(R, \phi) \in \mathbb{SO}(3) \times \mathbb{R}^3$, which is equivalent in coordinates but less intrinsic, and does not directly highlight the invariance properties of the SE(3) approach. The current modeling approach is motivated by easier accessibility for non-specialists, compatibility with classical coordinate-based approaches, and convenience in terms of handling external fields.

The equilibrium state of a beam is characterized by a still line of centroids and still cross-sections. Therefore, the equilibrium configuration is one such that the forces acting on each centroid and the torques on each cross-section balance out. In formal terms, equilibrium is achieved provided that

$$\begin{cases} \epsilon = R^\top \mathrm{d}_x \phi, \ \Gamma = R^\top \mathrm{d}_x R, \\ \mathrm{d}_x(R\, n) - g\varrho_0\, \mathrm{e}_\mathrm{z} + \varrho_0\, (\mathrm{d}_\phi b)^\top R\, m + f = 0, \\ \mathrm{d}_x M + [\Gamma, M] + \sigma(n\epsilon^\top) + \varrho_0\, \sigma(m\, b^\top R) + \Theta = 0, \end{cases} \tag{3.2}$$

where all dependent variables are functions of the spatial coordinate x only and the magnetic field is assumed to be time-invariant (otherwise, no balance may be achieved).

3.3. Mathematical modeling of friction

No mathematical model of a real mechanical system may be deemed complete without a term modeling friction, either internal–e.g., due to cross-sections sliding with respect to each other in a dense material–or external–e.g., friction with a fluid surrounding the beam, such as air or a liquid, as high-speed airflow results in significant friction.

There is no consensus in the specialized literature on how to model friction on a beam, as friction is a complex phenomenon that emerges from a combination of several effects. The recent contribution [4] extended the classical Timoshenko beam theory by introducing a micro-sliding variable that represents the average sliding across micro-cracks in cementitious materials. These micro-cracks are modeled as interacting rough surfaces (resembling interlocked teeth), which exhibit both the elastic deformation of asperities and frictional dissipation. The governing equations are derived via a variational Hamilton–Rayleigh approach, including elastic energy, external work, and a Rayleigh dissipation potential combining viscous and Coulomb-type friction effects.

In the present endeavor, we chose to recall the model discussed in [40, Section 2.2], based on a quadratic Rayleigh potential

$$Z(\partial_t \epsilon, \partial_t \Gamma) := \tfrac{1}{2}(\partial_t \epsilon)^\top F\, \partial_t \epsilon + \tfrac{1}{2}\mathrm{tr}((\partial_t \Gamma)^\top G\, \partial_t \Gamma), \tag{3.3}$$

where F, G denote the viscoelastic material's parameters. As in the previous case, the matrix G referred to in the equation above denotes a nonstandard version of the torsional viscoelastic friction tensor. The damping force and torque are related to the Rayleigh potential by the relations

$$\frac{\partial Z}{\partial\, \partial_t \epsilon} = F\, \partial_t \epsilon, \;\; \frac{\partial Z}{\partial\, \partial_t \Gamma} = \sigma(G\, \partial_t \Gamma), \tag{3.4}$$

respectively, which may be easily generalized by choosing any appropriate expression for the Rayleigh function. We can mention that the authors of [4] argued that linear damping underestimates the effect of friction in beam dynamics.

3.4. Energy exchange

In general, a beam exchanges energy with its surroundings. In order to quantify the rate of energy exchange, one may first want to define a total energy content

$$H(t) := \int_0^\ell K(x,t)\,\mathrm{d}x + \int_0^\ell E(x,t)\,\mathrm{d}x + \int_0^\ell U(x,t)\,\mathrm{d}x \tag{3.5}$$

as a function of time, and then evaluate the power exchange rate $\mathrm{d}_t H$, which quantifies the speed at which energy flows into or out of the beam. Apparently, the total energy density per single section cannot be expected to be conserved, not even in the case of a beam that does not exchange energy with its surrounding, since each section exchanges energy with nearby sections anyway. As a reference, readers might want to consult the review paper [13] and, in particular, Theorem 3.1 therein. The following paragraphs present a breakdown of each power contribution, whose calculation is based on the equations of motion written in the form (3.1).

For the kinetic energy component, it holds that

$$\begin{aligned}
\frac{\mathrm{d}}{\mathrm{d}t}\int_0^\ell K(x,t)\,\mathrm{d}x = &\int_0^\ell (\partial_t\phi)^\top \partial_x(R\,n)\,\mathrm{d}x - g\int_0^\ell \varrho_0\,(\partial_t\phi)^\top \mathrm{e}_z\,\mathrm{d}x \\
&+ \int_0^\ell \varrho_0\,(\partial_t\phi)^\top(\partial_\phi b)^\top R\,m\,\mathrm{d}x + \int_0^\ell (\partial_t\phi)^\top f\,\mathrm{d}x \\
&- \int_0^\ell \mathrm{tr}(\Omega^\top[\Omega,\Pi])\,\mathrm{d}x + \int_0^\ell \mathrm{tr}(\Omega^\top\partial_x M)\,\mathrm{d}x \\
&+ \int_0^\ell \mathrm{tr}(\Omega^\top[\Gamma, M])\,\mathrm{d}x + \int_0^\ell \mathrm{tr}(\Omega^\top\sigma(n\epsilon^\top))\,\mathrm{d}x \\
&- \int_0^\ell \varrho_0\,\mathrm{tr}(\Omega^\top\sigma(mb^\top R))\,\mathrm{d}x + \int_0^\ell \mathrm{tr}(\Omega^\top\Theta)\,\mathrm{d}x.
\end{aligned} \tag{3.6}$$

The first integral on the right-hand side may be rewritten, through integration by parts, as

$$\int_0^\ell (\partial_t\phi)^\top \partial_x(R\,n)\,\mathrm{d}x = (\partial_t\phi)^\top R\,n\big|_{x=0}^{x=\ell} - \int_0^\ell (\partial_{xt}\phi)^\top R\,n\,\mathrm{d}x. \tag{3.7}$$

The fifth integral on the right-hand side of the expression (3.6) is identically zero. The sixth integral on the right-hand side may be recast, again through integration by parts, as

$$\int_0^\ell \mathrm{tr}(\Omega^\top\partial_x M)\,\mathrm{d}x = \mathrm{tr}(\Omega^\top M)\big|_{x=0}^{x=\ell} - \int_0^\ell \mathrm{tr}(\partial_x\Omega^\top M)\,\mathrm{d}x. \tag{3.8}$$

As a consequence, the kinetic-type power reads as follows:

$$\begin{aligned}\frac{\mathrm{d}}{\mathrm{d}t}\int_0^\ell K(x,t)\,\mathrm{d}x = \ & (\partial_t\phi)^\top R\,n\big|_{x=0}^{x=\ell} - \int_0^\ell (\partial_{xt}\phi)^\top R\,n\,\mathrm{d}x - g\int_0^\ell q^\top \mathrm{e}_z\,\mathrm{d}x \\ & + \int_0^\ell q^\top(\partial_\phi b)^\top R\,m\,\mathrm{d}x + \int_0^\ell (\partial_t\phi)^\top f\,\mathrm{d}x + \operatorname{tr}(\Omega^\top M)\big|_{x=0}^{x=\ell} \\ & - \int_0^\ell \operatorname{tr}(M^\top\partial_x\Omega)\,\mathrm{d}x + 2\int_0^\ell \operatorname{tr}(M\,\Gamma\,\Omega)\,\mathrm{d}x + \int_0^\ell n^\top\Omega\,\epsilon\,\mathrm{d}x \\ & + \int_0^\ell \varrho_0\,b^\top R\,\Omega\,m\,\mathrm{d}x + \int_0^\ell \operatorname{tr}(\Omega^\top\Theta)\,\mathrm{d}x.\end{aligned} \tag{3.9}$$

Regarding the elastic energy component, it holds that

$$\frac{\mathrm{d}}{\mathrm{d}t}\int_0^\ell E(x,t)\,\mathrm{d}x = \int_0^\ell n^\top\partial_t\epsilon\,\mathrm{d}x + \int_0^\ell \operatorname{tr}(M^\top\partial_t\Gamma)\,\mathrm{d}x. \tag{3.10}$$

It pays to notice that

$$\begin{cases} n^\top\partial_t\epsilon = -n^\top\Omega\,\epsilon + (\partial_{tx}\phi)^\top R\,n, \\ \operatorname{tr}(M^\top\partial_t\Gamma) = 2\operatorname{tr}(M\,\Gamma\,\Omega) + \operatorname{tr}(M^\top\partial_x\Omega). \end{cases} \tag{3.11}$$

Therefore, the elastic-type power reads as follows:

$$\begin{aligned}\frac{\mathrm{d}}{\mathrm{d}t}\int_0^\ell E(x,t)\,\mathrm{d}x = \ & -\int_0^\ell n^\top\Omega\,\epsilon\,\mathrm{d}x + \int_0^\ell (\partial_{tx}\phi)^\top R\,n\,\mathrm{d}x \\ & - 2\int_0^\ell \operatorname{tr}(M\,\Gamma\,\Omega)\,\mathrm{d}x + \int_0^\ell \operatorname{tr}(M^\top\partial_x\Omega)\,\mathrm{d}x.\end{aligned} \tag{3.12}$$

In addition, for the external potential energy component, it holds that

$$\begin{aligned}\frac{\mathrm{d}}{\mathrm{d}t}\int_0^\ell U(x,t)\,\mathrm{d}x = \ & g\int_0^\ell q^\top \mathrm{e}_z\,\mathrm{d}x - \int_0^\ell q^\top(\partial_\phi b)^\top R\,m\,\mathrm{d}x \\ & - \int_0^\ell \varrho_0\,b^\top R\,\Omega\,m\,\mathrm{d}x - \int_0^\ell \varrho_0\,(\partial_t b)^\top R\,m\,\mathrm{d}x.\end{aligned} \tag{3.13}$$

The total energy rate is obtained upon summing up the three contributions (3.9), (3.12), and (3.13). As expected, most terms in the sum cancel out, as most of the energy exchange phenomena are conservative, as long as the solutions to the beam equations are smooth enough, namely $\partial_{tx}\phi = \partial_{xt}\phi$ and $\partial_{tx}\Omega = \partial_{xt}\Omega$ over the whole domain. The resulting expression for the total power thus reads

$$\begin{aligned}\mathrm{d}_t H = \ & (\partial_t\phi)^\top R\,n\big|_{x=0}^{x=\ell} + \operatorname{tr}(\Omega^\top M)\big|_{x=0}^{x=\ell} + \int_0^\ell (\partial_t\phi)^\top f\,\mathrm{d}x \\ & + \int_0^\ell \operatorname{tr}(\Omega^\top\Theta)\,\mathrm{d}x - \int_0^\ell \varrho_0\,(\partial_t b)^\top R\,m\,\mathrm{d}x.\end{aligned} \tag{3.14}$$

The five terms on the right-hand side may be given a clear physical interpretation. The first two terms represent the power input at the boundary: As these terms involve velocities, they might entail the

absorption of external energy into the beam or release of energy into the environment. The next two terms represent the work rate pertaining to the external forces and torques, while the last term in the summation represents the work rate due to a time-variable magnetic field.

The elastic-type power pertaining to the constraints on the ends of the beam may be zero under particular conditions. The term $(\partial_t \phi)^\top R\, n\big|_{x=0}^{x=\ell}$ may be zero if the ends are clamped (in which case $\partial_t \phi(0,t) = \partial_t \phi(\ell,t) = 0$ at any time) or if the cross-sections stay perpendicular to the centerline at the endpoints, in which case, $n(0,t) = n(\ell,t) = 0$, as explained in Section 2.7. Likewise, the term $\operatorname{tr}(\Omega^\top M)\big|_{x=0}^{x=\ell}$ may be zero in the case of clamped ends, which entails $\Omega(0,t) = \Omega(\ell,t) = 0$, or if the end sections are not subjected to any bending nor torsion, therefore $M(0,t) = M(\ell,t) = 0$, as also explained in Section 2.7.

The magnetic-type power pertaining to the magnetic field impinging the beam may be zero if the field does not depend explicitly on time, namely $\partial_t b = 0$. If, in addition, there are no external forces nor torques acting on the beam, i.e.. the motion is completely free except for gravity, then the energy of the beam is conserved, namely $H(t) =$ constant.

The energy-preserving properties demonstrated above have motivated the development of specialized numerical integrators that maintain these conservation laws at the discrete level. Recent work by [29] has shown that adaptive time-stepping strategies can be employed while preserving energy exactly, a property that is crucial for long-term stability in simulations of beam dynamics. The multisymplectic structure inherent in the Lie group formulation also enables the construction of integrators that preserve multiple conservation laws simultaneously [42].

3.5. Momentum exchange

The translational momentum density q is measured with respect to the inertial reference frame; therefore, the total translational momentum of a beam is defined as

$$\bar{q}(t) := \int_0^\ell q(x,t)\,\mathrm{d}x. \tag{3.15}$$

According to the equations of motion (3.1), the total translational momentum evolves as follows:

$$\partial_t \bar{q} = R\, n\big|_{x=0}^{x=\ell} - g\,\mathrm{e}_\mathrm{z} \int_0^\ell \varrho_0\,\mathrm{d}x + \int_0^\ell \varrho_0\,(\partial_\phi b)^\top R\, m\,\mathrm{d}x + \int_0^\ell f\,\mathrm{d}x. \tag{3.16}$$

Therefore, the beam exchanges translational momentum with the gravitational and magnetic fields, with the constraints at its ends and with any additional mechanical force. The total translational momentum is therefore conserved if all these forces are absent, in other words, when $f \equiv 0$, the field b is uniform across the beam, the gravitational constant $g \equiv 0$, and the two surfaces delimiting the beam are not subjected to bending. If these forces are acting on a beam but, taken as a whole, are in equilibrium, the translational momentum is conserved as well. This dynamic condition is the counterpart of the static condition expressed by the first of the Eq (3.2).

The evaluation of the total rotational momentum is more subtle. We first observe that the function $\Pi(x,t)$ represents the angular momentum of each section, which cannot be combined directly with other momenta, since each rotational momentum of this kind is in reference to a local (section-fixed) reference frame. In addition, the beam as a whole may be moving with respect to the inertial frame,

and hence a global momentum (similar to the orbital momentum of the Earth with respect to a Sun-centered reference system) must be taken into account. Therefore, the total angular momentum of a flexible beam is defined as

$$\bar{\Pi} := \int_0^\ell R\,\Pi\,R^\top\,\mathrm{d}x + \int_0^\ell \sigma(q\,\phi^\top)\,\mathrm{d}x, \tag{3.17}$$

where the first integral represents the total cross-sectional rotational momentum of the beam as seen from the inertial reference frame, while the second integral represents the resultant angular momentum of all centroids about the origin of the inertial reference system.

It is useful to recall the following identities, which arise from the definition of the involved variables and their properties:

$$\begin{cases} \partial_t(R\Pi R^\top) = R(\partial_t\Pi + [\Omega,\Pi])R^\top, \\ \partial_x(RMR^\top) = R(\partial_x M + [\Gamma, M])R^\top, \\ \partial_t\sigma(q\,\phi^\top) = \sigma((\partial_t q)\,\phi^\top), \\ R\sigma(n\epsilon^\top)R^\top = \sigma(R\,n\,\partial_x\phi^\top), \\ R\sigma(mb^\top R)R^\top = \sigma(R\,mb^\top). \end{cases} \tag{3.18}$$

The time-derivative of the total rotational momentum associated to the beam reads as follows:

$$\partial_t\bar{\Pi} = \int_0^\ell R(\partial_t\Pi + [\Omega,\Pi])R^\top\,\mathrm{d}x + \int_0^\ell \sigma(\partial_t q\,\phi^\top)\,\mathrm{d}x \tag{3.19}$$

whereby, substituting the equations of motion (3.1), it follows that

$$\begin{aligned} \partial_t\bar{\Pi} = &\int_0^\ell \partial_x(RMR^\top)\,\mathrm{d}x + \int_0^\ell \sigma(R\,n\,\partial_x\phi^\top)\,\mathrm{d}x - \int_0^\ell \varrho_0\,\sigma(R\,m\,b^\top)\,\mathrm{d}x \\ &+ \int_0^\ell \sigma(\partial_x(R\,n)\,\phi^\top)\,\mathrm{d}x - g\int_0^\ell \varrho_0\,\sigma(\mathrm{e}_z\,\phi^\top)\,\mathrm{d}x + \int_0^\ell \varrho_0\,\sigma((\partial_\phi b)^\top R\,m\,\phi^\top)\,\mathrm{d}x \\ &+ \int_0^\ell R\Theta R^\top\,\mathrm{d}x + \int_0^\ell \sigma(f\,\phi^\top)\,\mathrm{d}x. \end{aligned} \tag{3.20}$$

Applying the formula of integration by parts to the first two integrals on the right-hand side of the expression above, yields

$$\int_0^\ell \partial_x(RMR^\top)\,\mathrm{d}x = (RMR^\top)\big|_{x=0}^{x=\ell}, \tag{3.21}$$

$$\int_0^\ell \sigma(R\,n\,\partial_x\phi^\top)\,\mathrm{d}x = (R\,n\,\phi^\top)\big|_{x=0}^{x=\ell} - \int_0^\ell \sigma(\partial_x(R\,n)\,\phi^\top)\,\mathrm{d}x. \tag{3.22}$$

As a consequence, the total rotational momentum exchange rate reads as follows:

$$\begin{aligned} \partial_t\bar{\Pi} = &\,(RMR^\top)\big|_{x=0}^{x=\ell} + (R\,n\,\phi^\top)\big|_{x=0}^{x=\ell} + \int_0^\ell R\Theta R^\top\,\mathrm{d}x + \int_0^\ell \sigma(f\,\phi^\top)\,\mathrm{d}x \\ &- g\int_0^\ell \varrho_0\,\sigma(\mathrm{e}_z\,\phi^\top)\,\mathrm{d}x - \int_0^\ell \varrho_0\,\sigma(R\,m\,b^\top)\,\mathrm{d}x + \int_0^\ell \varrho_0\,\sigma((\partial_\phi b)^\top R\,m\,\phi^\top)\,\mathrm{d}x. \end{aligned} \tag{3.23}$$

In the case of a free beam ($m \equiv 0$, $\Theta \equiv 0$, $f \equiv 0$, $g \equiv 0$) with free edges ($\Gamma(0,t) = \Gamma(\ell,t) = 0$ and $\epsilon(0,t) = \epsilon(\ell,t) = \mathrm{e_x}$), each term on the right-hand side vanishes identically and hence the total angular momentum is conserved. Once again, momentum conservation may also arise when all the above terms are in equilibrium as a whole.

A constant $\bar{\Pi}$ still allows plenty of movements to the beam. If parts of the beam move internally (e.g., bend or twist), the rest of the beam may need to move in response in order to keep that total angular momentum fixed. (This phenomenon resembles that of a 'falling cat' [18]. A cat dropped upside down can reorient itself mid-air and land on its feet without any external torque as a result of bending and twisting its body, redistributing angular momentum internally.) If, for instance, a beam is free-floating (not fixed to a wall or the ground) and it undergoes internal motion-like nonuniform bending, torsion, or oscillation, this can lead to a net displacement or rotation of the whole beam. This effect is especially prominent in space structures (where there is no gravity or friction, such as satellites with extendable arms), soft robotics, and biological systems (like swimming worms or snakes [30], as well as in diving or gymnastic maneuvers [25]).

3.6. Length of a stretched beam

The constant ℓ can be interpreted as 'the length of a beam' (in fact, of its centerline) while undeformed. The length of a beam in a deformed state may be defined and evaluated as

$$\bar{\ell}(t) := \int_0^\ell \|\partial_x \phi(x,t)\| \, \mathrm{d}x \tag{3.24}$$

namely, using the standard rectification formula. As the beam deforms, the length $\bar{\ell}$ changes. The rate of change in the beam's length may be evaluated in terms of the strain change rate. In fact, upon noting that $\|\epsilon\| \equiv \|\partial_x \phi\|$, it may be readily seen that

$$\bar{\ell} = \int_0^\ell \|\epsilon\| \, \mathrm{d}x \quad \Rightarrow \quad \partial_t \bar{\ell} = \int_0^\ell \frac{\epsilon^\top \partial_t \epsilon}{\|\epsilon\|} \, \mathrm{d}x. \tag{3.25}$$

The ratio $\epsilon/\|\epsilon\|$ denotes the unit tangent vector to the centerline at a given location x, denoted as

$$\hat{\tau} := \frac{\partial_x \phi}{\|\partial_x \phi\|} \equiv \frac{\epsilon}{\|\epsilon\|}. \tag{3.26}$$

Therefore, the rate of change in the length of a beam may be expressed as

$$\partial_t \bar{\ell} = \int_0^\ell \hat{\tau}^\top \partial_t \epsilon \, \mathrm{d}x. \tag{3.27}$$

The expression above shows that the rate of stretching of the centerline depends solely on the tangential component of the change rate of the strain. An equivalent way to express the same quantity is

$$\partial_t \bar{\ell} = \int_0^\ell \hat{\tau}^\top \partial_x (\partial_t \phi) \, \mathrm{d}x, \tag{3.28}$$

which shows that the rate at which the beam stretches depends solely on the velocity gradient projected along the local tangent direction. Once again, it should be emphasized that the motion of a beam section is a combination of internal/local motion and of collective motion, as already discussed regarding the exchange of angular momentum.

4. Relations to simpler models

The geometrically exact three-dimensional beam theory, which is valid for extensive deformations of a beam as described in the previous section, is the product of intensive research, extending over decades, which includes simpler models. In the present section, we discuss the relationships between the general geometrically exact model and the simpler ones it encompasses.

4.1. Special instances

Special cases of the equations of motion (2.43) may be derived under appropriate assumptions. In some cases of interest, the reduced equations of motion are solvable in closed form.

Free elastic beam – An interesting special case that offers some insight into the dynamic behavior is that of a free beam, namely one that is neither subjected to any external force or torque. In this case, the equations of dynamics (2.43) simplify to

$$\begin{cases} \varrho_0\, \partial_{tt}\phi = \partial_x(RC(\epsilon - \mathrm{e_x})), \\ \sigma(J\partial_t\Omega) - \sigma(J\Omega^2) = \partial_x\sigma(D\Gamma) - \sigma(D\Gamma^2) + \sigma(C(\epsilon - \mathrm{e_x})\epsilon^\top). \end{cases} \tag{4.1}$$

The partial differential equations above describe the paired motion of the line of centroids and of each cross-section due uniquely to the internal elastic forces and torques. Starting from a nonequilibrium condition, the internal forces/torque tend to make the beam bend and twist and, in the absence of dissipation phenomena, to do so indefinitely. In fact, both equations resemble a wave equation, as will be even more apparent in the next example.

Elastic string – A very thin rod or filament may be modeled as a string, assuming that the torsion of the beam is negligible. Formally, this case corresponds to the assumption that $R(x,t) = I_3$ for any $(x,t) \in [0,\ \ell] \times [0,\ T]$, where I_3 denotes an identity matrix. In addition, we assume that $C = Y\,A\,I_3$, with $Y > 0$ denoting a constant Young's modulus, that the mass density $\varrho > 0$, that the cross-section areas A are constant, that the magnetic field is uniform, and that no further external forces act on the beam. Under these assumptions, the equations of motion (2.43) simplify to

$$\partial_{tt}\phi = \tfrac{Y}{\varrho}\partial_{xx}\phi - g\,\mathrm{e_z} \tag{4.2}$$

where the linear density ϱ equals just the ratio of the total mass of the string over its length.

Whenever the effect of the gravitational field can be neglected ($g \equiv 0$), the x- and y-coordinate of the string follow a wave equation, where the quantity $\sqrt{Y/\varrho}$ determines the speed of the stress wave (which is notoriously higher in stiffer and thinner materials). Boundary conditions may be set up in such a way for the string to be open-ended or closed, in which case, it forms a loop. The equilibrium configuration of a string may be computed by solving the purely spatial equation $\frac{\mathrm{d}^2\phi}{\mathrm{d}x^2} = \frac{g\varrho}{Y}\mathrm{e_z}$, whose solution may be expressed as a second-order polynomial in the variable x.

Unbound beam – A case-limit of study may be considered by setting the stiffness of the beam to zero, namely by setting $C = D = 0$. In this case, it is not hard to guess the outcome: Since the bonding energy vanishes, each cross-section becomes unbound from its neighbors and the beam loses its shape

(much like a liquid) and falls apart. The equations of motion, in fact, become

$$\begin{cases} \partial_t R = R\,\Omega, \\ \varrho_0\,\partial_{tt}\phi + g\varrho_0\,\mathrm{e}_\mathrm{z} - \varrho_0\,\partial_\phi^\top b\,R\,m = f, \\ \sigma(J\partial_t\Omega) - \sigma(J\Omega^2) - \varrho_0\,\sigma(m\,b^\top R) = \Theta. \end{cases} \tag{4.3}$$

Since the elastic bonding force vanished, each section rotates and translates in space on its own, according to the gravitational pull, magnetic force, and torque. Notice that, in the present case-limit, the equations of motion are coupled only by the magnetic-type terms and possibly by the external forces/torques. Therefore, in the absence of these terms, the equation of motion of the centroids and the equations of rotation of the cross-section are independent from one another.

The framework presented in this survey has been extended to address various specialized applications. Notable developments include the treatment of beams with embedded strong discontinuities for modeling structural failure [67], which maintains the geometrically exact nature while incorporating damage mechanics. Additionally, recent work has focused on eliminating shear locking phenomena through sophisticated interpolation schemes based on unit dual quaternions [42], addressing a long-standing numerical challenge in beam-related finite element implementations.

4.2. Geometrically exact, three-dimensional Euler-Bernoulli beams

An analysis of the specialized literature (see, e.g., [19, Section 6]) reveals that the Euler-Bernoulli beam theory does not arise as a special case of the geometrically exact Simo-Reissner theory. In fact, to get the equations of motion postulated by Euler and Bernoulli, it is necessary to modify the variational formulation by including constraints that ultimately affect the structure of the equations of motion. Such constraints are non-holonomic – in the sense that they set bounds on the derivatives of the independent variables, in contrast to holonomic constraints that bind the independent variables directly – and are often managed by the Lagrange multiplier method [19]. In a differential-geometric setting, non-holonomic constraints might, however, be treated via the notion of distribution, which serves to express constraints on the tangent bundle associated with the configuration space of a beam system (see, e.g., [9]).

Nonlinear Euler-Bernoulli beam theory – In a nonlinear Euler-Bernoulli beam, it is assumed that each cross-section stays orthogonal to the centerline. This requirement imposes constraints on the product $R^\top\partial_x\phi$. Upon introducing a further director vector e_y such that $[\mathrm{e}_\mathrm{x}\ \mathrm{e}_\mathrm{y}\ \mathrm{e}_\mathrm{z}] = I_3$, the non-linear Euler-Bernoulli beam constraints read [19, Section 6.1]

$$\mathrm{e}_\mathrm{y}^\top(R^\top\partial_x\phi) = \mathrm{e}_\mathrm{z}^\top(R^\top\partial_x\phi) = 0 \tag{4.4}$$

to hold at all points along a beam and at all moments in time. Since the product $R^\top\partial_x\phi$ denotes the tangent to the centerline expressed in the inertial reference frame, the two conditions above ensure that the beam's centerline is always aligned with the local material x-axis, thereby ensuring unshearability consistent with the Euler-Bernoulli assumption. In a non-linear Euler-Bernoulli beam, however, the quantity $\mathrm{e}_\mathrm{x}^\top(R^\top\,\partial_x\phi)$ stays free, as it depends on how the beam stretches along its own centerline, as already discussed in Section 3.6.

An inextensible non-linear Euler-Bernoulli beam model obtained via the notion of distribution – Cantilever and free-ends beams are essentially inextensible [17]. In general, a beam is inextensible

when its centerline does not stretch under deformation. In an inextensible non-linear Euler-Bernoulli beam model, in addition to the conditions (4.4), it is assumed that

$$\mathrm{e_x}^\top (R^\top \partial_x \phi) = 1 \tag{4.5}$$

at all time instants and at all spatial points along a beam. In several contributions, the inextensibility condition is formulated as $\|\partial_x \phi\| = 1$. This condition, together with the constraints (4.4), and the physically reasonable assumption that [19] $\mathrm{e_x}^\top (R^\top \partial_x \phi) > 1$, are equivalent to the vector constraint

$$\partial_x \phi(x,t) = R(x,t)\,\mathrm{e_x} \tag{4.6}$$

to hold at all times and everywhere along the beam. The constraint (4.6) is equivalent to $n(x,t) \equiv 0$ anytime, everywhere along the beam. A further observation is that the condition (4.6) constraints the shape of the centerline to be entirely determined by the rotation field $R(x,t)$. In fact, upon spatial integration it is immediate to see that

$$\phi(x,t) = \phi(0,t) + \int_0^x R(\xi,t)\,\mathrm{e_x}\,\mathrm{d}\xi. \tag{4.7}$$

The relation above is the consequence of the fact that, in an inextensible beam, neither stretching nor shear happen, and hence the shape of the centerline only depends on the way the cross-sections are oriented along the beam.

By computing the variation of the inextensibility constraint, namely by applying the operator $\partial_s|_{s=0}$ to both sides of the relation (4.6), one gets the differential constraint on the variations

$$\partial_x(\delta\phi) = R(\delta R)\mathrm{e_x}, \tag{4.8}$$

having assumed the function ϕ to be smooth enough to warrant the commutativity of δ with ∂_x. This relation binds the variations δR and $\delta\phi$ to one another. Technically, this operation defines a distribution $\mathbb{D} \subset \mathrm{T}(\mathbb{SO}(3) \times \mathbb{R}^3)$ such that each variation $(\delta R, \delta\phi) \in \mathbb{D}$ must belong to.

In order to formulate the equations of motion for a full three-dimensional Euler-Bernoulli beam, we make some simplifications that do not hinder generality. The first simplification consists of assuming that the elastic energy of the beam coincides with the torsional elastic energy only. The second simplification consists of ignoring the external potential energy U and assuming that all forcing terms in the equations are summarized in the torque field Θ. The Lagrangian function that describes the dynamics of the beam hence simplifies to

$$L_\mathrm{c}(x,t) := \tfrac{1}{2}\varrho_0(x)\|\partial_t\phi(x,t)\|^2 + \tfrac{1}{2}\mathrm{tr}(\Omega^\top(x,t)J(x)\Omega(x,t)) - \tfrac{1}{2}\mathrm{tr}(\Gamma^\top(x,t)D(x)\Gamma(x,t)), \tag{4.9}$$

where the subscript 'c' stands for 'constrained'.

The variation of the constrained Lagrangian reads as follows:

$$\delta L_\mathrm{c} = \varrho_0(\partial_t\phi)^\top \partial_t(\delta\phi) + \mathrm{tr}(\Omega^\top J\,\delta\Omega) - \mathrm{tr}(\Gamma^\top D\,\delta\Gamma), \tag{4.10}$$

where the variations of the dependent variables take the expressions

$$\begin{cases} \delta\Omega = \Omega\,\delta R - \delta R\,\Omega + \partial_t(\delta R), \\ \delta\epsilon = -\delta R\,\epsilon + \delta R\,\mathrm{e_x}, \\ \delta\Gamma = \Gamma\,\delta R - \delta R\,\Gamma + \partial_x(\delta R). \end{cases} \tag{4.11}$$

Plugging these expressions into the variation of the constrained Lagrangian (4.10) and integrating with respect to the temporal and spatial variable yields the variation-of-action terms

$$\begin{aligned}\int_0^\ell \int_0^T \varrho_0\,(\partial_t\phi)^\top \partial_t(\delta\phi)\,\mathrm{d}t\,\mathrm{d}x &= -\int_0^T \int_0^\ell \varrho_0\,(\partial_{tt}\phi)^\top \delta\phi\,\mathrm{d}x\,\mathrm{d}t \\ &= \int_0^T \int_0^\ell \int_0^x \varrho_0(\xi)(\partial_{tt}\phi(\xi,t))^\top \mathrm{d}\xi\, R(x,t)\,\delta R(x,t)\,\mathrm{e_x}\,\mathrm{d}x\,\mathrm{d}t \\ &= \int_0^T \int_0^\ell \mathrm{tr}\left(\sigma\left(\mathrm{e_x}\int_0^x \varrho_0\,(\partial_{tt}\phi)^\top \mathrm{d}\xi\, R\right)\delta R\right)\mathrm{d}x\,\mathrm{d}t,\end{aligned} \tag{4.12}$$

where we have used the initial/final conditions $\delta\phi(x,0) = \delta\phi(x,T) = 0$ and the boundary conditions $\delta\phi(0,t) = \delta\phi(\ell,t) = 0$ to eliminate tail terms [17],

$$\begin{aligned}\int_0^\ell \int_0^T \mathrm{tr}(\Omega^\top J\,\delta\Omega)\,\mathrm{d}t\,\mathrm{d}x &= -\int_0^\ell \int_0^T \mathrm{tr}(\Omega J(\Omega\,\delta R - \delta R\,\Omega + \partial_t(\delta R)))\,\mathrm{d}t\,\mathrm{d}x \\ &= \int_0^\ell \int_0^T \mathrm{tr}(\sigma(\Omega^2 J + \partial_t\Omega J)\,\delta R)\,\mathrm{d}t\,\mathrm{d}x,\end{aligned} \tag{4.13}$$

where we have used the initial/final conditions $\delta R(x,0) = \delta R(x,T) = 0$ and the fact that $\mathrm{tr}(\Omega^\top J\,\Omega\,\delta R) \equiv 0$, and

$$\int_0^\ell \int_0^T \mathrm{tr}(\Gamma^\top D\,\delta\Gamma)\,\mathrm{d}t\,\mathrm{d}x = \int_0^T \int_0^\ell \mathrm{tr}(\sigma(\Gamma^2 D + \partial_x(\Gamma D))\,\delta R)\,\mathrm{d}x\,\mathrm{d}t, \tag{4.14}$$

where we have used the boundary condition $\Gamma(0,t)D(0)\delta R(0,t) = \Gamma(\ell,t)D(\ell)\delta R(\ell,t)$ and the fact that $\mathrm{tr}(\Gamma^\top D\,\Gamma\,\delta R) \equiv 0$.

As a result, the variation of the constrained action reads

$$\int_0^T \int_0^\ell \delta L_\mathrm{c}\,\mathrm{d}x\,\mathrm{d}t = \int_0^T \int_0^\ell \mathrm{tr}(P^\top \delta R)\,\mathrm{d}x\,\mathrm{d}t, \tag{4.15}$$

where the field $P(x,t) \in \mathfrak{so}(3)$ reads

$$P := \sigma(J\Omega^2 - J\partial_t\Omega) - \sigma(D\Gamma^2 - \partial_x(D\Gamma)) - \sigma\left(R^\top \int_0^x \varrho_0\,(\partial_{tt}\phi)\mathrm{d}\,\xi\,\mathrm{e_x}^\top\right). \tag{4.16}$$

By the assumptions made, the variational principle (2.12) simplifies to

$$\int_0^T \int_0^\ell \delta L_\mathrm{c}\,\mathrm{d}x\,\mathrm{d}t + \int_0^T \int_0^\ell \mathrm{tr}(\Theta^\top \delta R)\,\mathrm{d}x\,\mathrm{d}t = 0, \tag{4.17}$$

which leads to the single equation of (torsional) motion $P + \Theta = 0$. This equation may be further particularized by explicitly computing the expression of $\partial_{tt}\phi$. From the integral (4.7), it readily follows that

$$\partial_{tt}\phi(x,t) = \frac{\mathrm{d}^2\phi}{\mathrm{d}t^2}(0,t) + \int_0^x R(\xi,t)(\Omega^2(\xi,t) + \partial_t\Omega(\xi,t))\,\mathrm{e_x}\,\mathrm{d}\xi. \tag{4.18}$$

Therefore, the integral in the expression of P may be written explicitly in terms of the initial condition on ϕ as

$$\int_0^x \varrho_0\,(\partial_{tt}\phi)\,\mathrm{d}\,\xi = \int_0^x \varrho_0\,\mathrm{d}\xi\,\tfrac{\mathrm{d}^2\phi}{\mathrm{d}t^2}(0,t) + \int_0^x \varrho_0 \int_0^\xi R(\eta,t)(\Omega^2(\eta,t) + \partial_t\Omega(\eta,t))\,\mathrm{e_x}\,\mathrm{d}\eta\,\mathrm{d}\xi. \tag{4.19}$$

As a consequence, the geometrically exact equations of motion of an inextensible, fully three-dimensional, Euler-Bernoulli beam are

$$\begin{cases} \partial_t R = R\,\Omega,\ \Gamma = R^\top \partial_x R, \\ \phi(x,t) = \phi(0,t) + \int_0^x R\,\mathrm{e_x}\,\mathrm{d}\xi, \\ \sigma(J\Omega^2 - J\partial_t\Omega) - \sigma(D\Gamma^2 - \partial_x(D\Gamma)) - \sigma\left(\left(\int_0^x \varrho_0\,\mathrm{d}\xi\right) R^\top \dfrac{\mathrm{d}^2\phi}{\mathrm{d}t^2}(0,t)\,\mathrm{e_x}^\top\right) \\ -\sigma\left(R^\top \int_0^x \varrho_0 \int_0^\xi R(\eta,t)(\Omega^2(\eta,t) + \partial_t\Omega(\eta,t))\,\mathrm{d}\eta\,\mathrm{d}\xi\,\mathrm{e_x}\,\mathrm{e_x}^\top\right) + \Theta = 0. \end{cases} \tag{4.20}$$

Not surprisingly, these equations do not coincide with the general equations of motion (2.43), where one sets $n \equiv 0$. A mathematical model of this sort would be obtained by applying the constraint following the precepts of non-holonomic mechanics, in contrast to those commonly referred to as Kozlov's 'vakonomic mechanics'. These two approaches to mechanics are notoriously inequivalent to one another [43]. The Eq (4.20) has been written explicitly in the variable R (and thus also including $\Omega = R^\top \partial_t R$ and $\Gamma = R^\top \partial_x R$) so as to allow an easier comparison with the expression (32) in [17].

The first and third equations in (4.20) are reconstruction relations that help in calculating the actual position of the centerline and rotation of each cross-section. The third equation, in particular, tells us that the shape of the centerline depends solely on the orientation of the cross-sections, as no tangential sliding is possible as an effect of inextensibility. The reason why the condition (4.6) is referred to as 'inextensibility' is quite apparent if one plugs this condition into the expression (3.24), which gives $\bar{\ell} = \ell$ at all time instants, showing that the length of a beam will not change despite deformation.

The equations of motion of a full 'three-dimensional inextensible Euler-Bernoulli beam', expressed in generalized coordinates, read

$$\begin{cases} q = \varrho_0\,\mathrm{d}_t\phi(0,t) + \varrho_0 \int_0^x R(\xi,t)\Omega(\xi,t)\,\mathrm{e_x}\,\mathrm{d}\xi, \\ \partial_t\Pi + [\Omega,\Pi] = \partial_x M + [\Gamma, M] + \sigma\left(R^\top \int_0^x \partial_t q\,\mathrm{e_x}^\top \mathrm{d}\xi\right) + \Theta. \end{cases} \tag{4.21}$$

Therefore, the equilibrium conditions for an inextensible Euler-Bernoulli beam are

$$\begin{cases} \Gamma = R^\top \mathrm{d}_x R, \\ \mathrm{d}_x M = [M,\Gamma] - \Theta, \\ \phi(x) = \phi(0) + \int_0^x R(\xi)\,\mathrm{e_x}\,\mathrm{d}\xi, \end{cases} \tag{4.22}$$

where $\phi(0)$ represents a stationary boundary condition and the total torque Θ is supposed to be stationary as well, namely $\Theta = \Theta(x)$. The first two relations in the system above might be, in fact, summarized by a second-order differential equation in the rotation field $R = R(x)$.

An inextensible nonlinear Euler-Bernoulli beam model obtained via the Lagrange multiplier method – In the present alternative derivation, we shall tackle the problem of modeling an inextensible non-linear Euler-Bernoulli beam by the usual method – in this context – of Lagrange multipliers, which are well known in the specialized literature [19]. For a theoretical review of this method in mechanics, see, e.g., [53]. Indeed, this approach introduces a physical variable, a Lagrange multiplier, that may be well interpreted in terms of beam dynamics. As underlined in [17], this approach is equivalent to that based on the notion of distribution and leads to the same results.

The method is based again on the constrained Lagrangian $L_c = L_c(\phi, \partial_t\phi, R, \partial_t R, \partial_x R)$ and consists of imposing the variational constraint $\partial_x(\delta\phi) = R(\delta R)\mathrm{e_x}$ via a Lagrange multiplier $\lambda \in \mathbb{R}^3$. Such an additional term appears in the variational principle as a sort of virtual work. Indeed, the principle (2.12) needs to be modified as

$$\int_0^T \int_0^\ell \delta L_c \,\mathrm{d}x\,\mathrm{d}t + \int_0^T \int_0^\ell \mathrm{tr}(\Theta^\top \delta R)\,\mathrm{d}x\,\mathrm{d}t + \int_0^T \int_0^\ell \lambda^\top(\partial_x(\delta\phi) - R\,\delta R\,\mathrm{e_x})\,\mathrm{d}x\,\mathrm{d}t = 0, \tag{4.23}$$

where the differential constraint arising from inextensibility is enforced in a *weak* form through the Lagrange multiplier.

As in the previous derivation, we have

$$\begin{aligned}\int_0^T \int_0^\ell \delta L_c \,\mathrm{d}x\,\mathrm{d}t = &-\int_0^T \int_0^\ell \varrho_0(\partial_{tt}\phi)^\top \delta\phi \,\mathrm{d}x\,\mathrm{d}t + \int_0^\ell \int_0^T \mathrm{tr}(\sigma(\Omega^2 J + \partial_t\Omega\, J)\,\delta R)\,\mathrm{d}t\,\mathrm{d}x \\ &- \int_0^T \int_0^\ell \mathrm{tr}(\sigma(\Gamma^2 D + \partial_x(\Gamma D))\,\delta R)\,\mathrm{d}x\,\mathrm{d}t.\end{aligned} \tag{4.24}$$

In addition, the double integral containing the Lagrange multiplier may be rewritten by observing that

$$\int_0^T \int_0^\ell \lambda^\top \partial_x(\delta\phi)\,\mathrm{d}x\,\mathrm{d}t = -\int_0^T \int_0^\ell \left(\frac{\partial\lambda}{\partial x}\right)^\top \delta\phi\,\mathrm{d}x\,\mathrm{d}t, \tag{4.25}$$

and

$$\int_0^T \int_0^\ell \lambda^\top R\,\delta R\,\mathrm{e_x}\,\mathrm{d}x\,\mathrm{d}t = \int_0^T \int_0^\ell \mathrm{tr}\left(\sigma(\mathrm{e_x}\,\lambda^\top R)\,\delta R\right)\,\mathrm{d}x\,\mathrm{d}t, \tag{4.26}$$

so that the terms in the variations $\delta\phi$ and δR may now be split in two equations of motion as follows:

$$\begin{cases}\varrho_0\,(\partial_{tt}\phi) + \partial_x\lambda = 0, \\ \sigma(J\Omega^2) - \sigma(J\partial_t\Omega) - \sigma(D\Gamma^2) + \partial_x\sigma(D\Gamma) + \sigma(R^\top\lambda\mathrm{e_x}^\top) + \Theta = 0.\end{cases} \tag{4.27}$$

The first equation reveals that λ is a force experienced by the bending beam and $\partial_x\lambda$ is a distributed force that creates inertia [17]. In other terms, the Lagrange multiplier is equivalent to the tension force introduced in the equations of motion, e.g., in inextensible cables.

The mathematical model (4.27) and the model (4.20) are equivalent. In fact, the Lagrange multiplier may be written in terms of the centerline function ϕ as

$$\lambda(x,t) = -\int_0^x \varrho(\xi)\,\partial_{tt}\phi(\xi,t)\,\mathrm{d}\xi \tag{4.28}$$

under the proviso that $\lambda(0,t) = 0$. Plugging this relation into the second equation in (4.27) yields the three-dimensional inextensible Euler-Bernoulli model (4.20).

Certainly, the exact form of the equations of motion for an inextensible beam depend on the boundary conditions, which enter the calculations in several places. A simple classification of these conditions, based on Section 2.2 of the paper [17], is proposed in Table 4. A cantilevered beam is one with a single end clamped, while a free-free beam is one with both ends free.

Table 4. Classification of boundary conditions.

Type of support	Kinematic condition
Clamped boundary	Both $\phi(0,t)$ and $R(0,t)$ fixed for any t
Pinned boundary	Only $\phi(0,t)$ fixed for any t
Free boundary	Neither $\phi(0,t)$ nor $R(0,t)$ fixed

4.3. Geometrically exact, planar beam model

Further beam models may be obtained by restricting the motion of the centerline to the x–z plane (recall that the x axis denotes the longitudinal direction of a beam, while the z axis is related to the direction of gravity) and the tilting of each one-dimensional cross-section relative to the y axis. In a planar model, the coordinate of each centroid is hence described by a function $\phi(x,t) \in \mathbb{R}^2$, and the orientation of each cross-section is described by a function $R(x,t) \in \mathrm{SO}(2)$ that represents a rotation along the y axis. An example of an undeformed and of a deformed two-dimensional beam are shown in Figure 2.

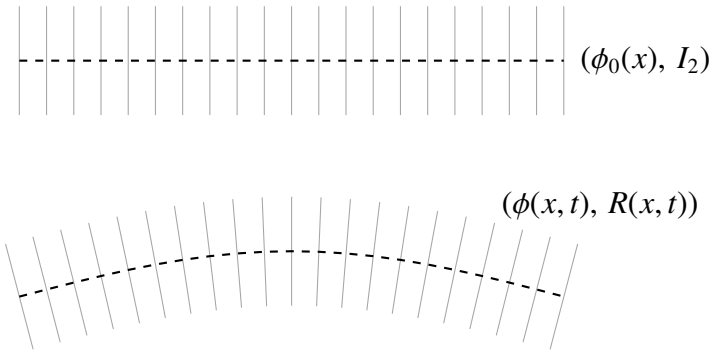

Figure 2. Schematic illustration of an undeformed and of a deformed two-dimensional Euler-Bernoulli beam.

On the basis of the settings above, it is not hard to see that the equations of the free motion in two dimensions of a geometrically exact flexible beam read as follows:

$$\begin{cases} \varrho_0\, \partial_{tt}\phi = C\, \partial_x(R(\epsilon - \mathrm{e_x})), \\ J\, \partial_t\Omega = D\, \partial_x\Gamma + C\sigma(\epsilon\, \mathrm{e_x}^{\top}) \end{cases} \tag{4.29}$$

where $J > 0$, $C > 0$ and $D > 0$ represent constant scalar coefficients, $\mathrm{e_x} \in \mathbb{R}^2$ denotes the unit vector associated to the x axis in two dimensions, $\Omega, \Gamma \in \mathfrak{so}(2)$, while $\epsilon \in \mathbb{R}^2$.

4.4. Linearized models

Linearization of the equations of motion of a beam may be performed, provided that the mathematical assumptions resulting from linearization are consistent with the physics of an actual object.

Linearization of a three-dimensional model of a free elastic beam including bending of the centerline and only torsion of cross sections – A first instance is derived from the model (4.1) by

introducing a number of assumptions. The main assumptions are: (a) each cross-section undergoes only moderate rotation about the longitudinal x-axis, and (b) the bending of the centerline is moderate. These assumptions translate into the mathematical approximations

$$\begin{cases} R(x,t) \approx I_3 + \theta(x,t)\,\mathrm{B_x}, \\ \phi(x,t) \approx \phi_0(x) + u(x,t), \end{cases} \tag{4.30}$$

where $\theta \in \mathbb{R}$ denotes a small rotation angle, $\mathrm{B_x} \in \mathfrak{so}(3)$ denotes the infinitesimal generator (that is, a skew-symmetric matrix) of a rotation around the x axis, ϕ_0 denotes the undeformed centerline of the beam, and $u \in \mathbb{R}^3$ denotes a deflection function such that both $\|u\|$ and $\|\partial_x u\|$ are small. In order to emphasize the linear character of the approximated equations of motion, we shall also assume that the stiffness matrices C and D are constant along the beam.

According to the first-order approximations (4.30), we get the following expressions:

$$\begin{cases} \Omega \approx \partial_t \theta\,\mathrm{B_x}, \\ \Gamma \approx \partial_x \theta\,\mathrm{B_x}, \\ \epsilon \approx \mathrm{e_x} + \partial_x u \end{cases} \tag{4.31}$$

motivated by the observation that $\sigma(\mathrm{B_x}^2) = 0$, $\partial_x \phi_0 = \mathrm{e_x}$, and by the decision to neglect all higher-order terms. As a consequence, it holds that

$$\begin{cases} \partial_x(RC(\epsilon - \mathrm{e_x})) \approx\ C\partial_{xx} u, \\ \partial_t \sigma(J\Omega) \approx \partial_t \theta\, J_x\, \mathrm{B_x}, \\ \partial_x \sigma(D\Gamma) \approx \partial_x \theta\, D_x\, \mathrm{B_x}, \\ \sigma(C(\epsilon - \mathrm{e_x})\epsilon^\top) \approx \sigma(C\,\partial_x u\,\mathrm{e_x}^\top), \end{cases} \tag{4.32}$$

where $J_x > 0$ denotes the inertia coefficient along the x axis, $D_x > 0$ denotes the torsional stiffness along the longitudinal direction, which are both assumed to be constant, and where we retain the coupling term between stretching and torsion represented by the torque $\sigma(C\partial_x u\,\mathrm{e_x}^\top)$. The resulting equations of motion turn out to be

$$\begin{cases} \varrho_0\,\partial_{tt} u = C\partial_{xx} u, \\ J_x \partial_t \theta = D_x \partial_x \theta + \mathrm{tr}(\mathrm{B_x}^\top \sigma(C\partial_x u\,\mathrm{e_x}^\top)), \end{cases} \tag{4.33}$$

where we have introduced a projection of the coupling torque onto the x axis so as to isolate the meaningful torsional component along this axis. The Eq (4.33) may be considered as a linearization of the equations of motion of a free three-dimensional beam.

Linearization of a two-dimensional model of a free elastic beam that leads to the classical Euler-Bernoulli equations – A second instance is derived from the two-dimensional model (4.29). Again, the main assumptions are that (a) the rotation of each cross-section is limited to the y-axis and remains moderate, and (b) the bending of the centerline is moderate. These assumptions translate into

$$\begin{cases} R(x,t) \approx I_2 + \theta(x,t)\,\mathrm{B_y}, \\ \phi(x,t) \approx \phi_0(x) + u(x,t)\,\mathrm{e_x} + w(x,t)\,\mathrm{e_z} \end{cases} \tag{4.34}$$

where $\theta \in \mathbb{R}$ now denotes a small tilting angle, $\mathrm{B_y} \in \mathfrak{so}(2)$ denotes the infinitesimal generator matrix of a rotation around the y axis in two dimensions, $\mathrm{e_z} \in \mathbb{R}^2$ denotes the vertical direction on the plane, and the function ϕ_0 again denotes the undeformed centerline of the beam. The function $u \in \mathbb{R}$ denotes the axial component of deformation (stretching), while the function $w \in \mathbb{R}$ denotes a vertical component of deformation (bending). It is assumed that $|u|$, $|w|$, $|\partial_x u|$, and $|\partial_x w|$ are small compared with the norm $\|\phi_0\|$.

According to the approximations (4.34), we obtain the following approximate expressions:

$$\begin{cases} \Omega \approx \partial_t \theta \, \mathrm{B_y}, \\ \Gamma \approx \partial_x \theta \, \mathrm{B_y}, \\ \epsilon \approx (1 + \partial_x u) \, \mathrm{e_x} + \partial_x w \, \mathrm{e_z} \end{cases} \tag{4.35}$$

since all terms of order higher than one were (and again will be) neglected. Therefore, the following approximations hold:

$$\begin{cases} \partial_x (RC(\epsilon - \mathrm{e_x})) \approx C(\partial_{xx} u \, \mathrm{e_x} + \partial_{xx} w \, \mathrm{e_z}), \\ J \, \partial_t \Omega \approx J \, \partial_{tt} \theta \, \mathrm{B_y}, \\ D \, \partial_x \Gamma \approx D \, \partial_x \theta \, \mathrm{B_y}, \\ C\sigma(\epsilon \, \mathrm{e_x}^\top) \approx C\sigma((\partial_x u \, \mathrm{e_x} + \partial_x w \, \mathrm{e_z})\mathrm{e_x}^\top) = \frac{C}{2} \, \partial_x w \, \mathrm{B_y}, \end{cases} \tag{4.36}$$

since $2\,\sigma(\mathrm{e_z e_x}^\top) = \mathrm{B_y}$. The approximate equations of motion then read

$$\begin{cases} \varrho_0 \, \partial_{tt} u = C \, \partial_{xx} u, \\ \varrho_0 \, \partial_{tt} w = C \, \partial_{xx} w, \\ J \, \partial_{tt} \theta = D \, \partial_{xx} \theta + \frac{C}{2} \partial_x w. \end{cases} \tag{4.37}$$

In the Euler-Bernoulli theory, there two further assumptions appear that allow one to condense the latter two equations into one. The first assumption is that each cross-section of the beam does not warp nor tilt independently, hence the rotation angle θ of a cross-section is entirely dependent on the bending of the beam; in particular, cross-sections remain perpendicular to the centerline, which leads to the geometric constraint

$$\theta = \partial_x w, \tag{4.38}$$

which is generally termed the 'geometric compatibility condition'. The second assumption is that the rotational inertia J is negligible (i.e., tilting happens instantaneously without any propagation delay–see, e.g., [5, Section 1]), namely one may set $J = 0$ in the equations. By way of these assumptions, the last relation in (4.37) gives $C \, \partial_{xx} w = -2 \, D \, \partial_{xxx} (\partial_x w)$, and hence the equations of motion for the longitudinal and vertical displacements take the form

$$\begin{cases} \varrho_0 \, \partial_{tt} u = C \, \partial_{xx} u, \\ \varrho_0 \, \partial_{tt} w = -2 \, D \, \partial_{xxxx} w \end{cases} \tag{4.39}$$

thereby looking like the classical Euler-Bernoulli equations for a flexible beam. In particular, the last equation represents the classical second-order in time, fourth-order in space, Euler-Bernoulli partial differential equation, which is well known in several disciplines, including robotics [68].

In the specialized literature on the classical Euler-Bernoulli equations, the equation governing bending is often written as $\varrho\, A\, w_{tt} + Y\, I\, w_{xxxx} = 0$, where the product YI denotes the flexural rigidity of the beam. Likewise, the axial displacement equation is often found in the form $\varrho\, A\, u_{tt} = C\, u_{xx}$. A comparison with the expressions (4.39) leads to the identifications $\varrho_0 \leftrightarrow \varrho A$, $C \leftrightarrow YA$, and $D \leftrightarrow \frac{1}{2} YI$. The latter two link the stiffness parameters to the material parameters.

In principle, it is straightforward to model complex phenomena, such as the motion of a vehicle over a flexible path, by coupling the Lagrangian of the vehicle with the Lagrangian of the beam through terms that describe their interaction (see, e.g., [68] and the references therein).

Linearization of the three-dimensional model, including bending of the centerline, twisting, and tilting of cross sections – A complete linearization of the mathematical model (3.1) which accommodates moderate bending, twisting, tilting, and gradient effects can be obtained by appropriate small-displacement approximations with respect to the neutral configuration (ϕ_0, I_3). Let us recall the relevant equations

$$\begin{cases} q = \varrho_0\, \partial_t \phi,\ \Pi = \sigma(J\Omega),\ n = C(\epsilon - \mathrm{e_x}),\ M = \sigma(D\Gamma), \\ \partial_t q = \partial_x (R\, n) - g \varrho_0\, \mathrm{e_z} + \varrho_0\, \partial_\phi^\top b\, R\, m + f, \\ \partial_t \Pi + [\Omega, \Pi] = \partial_x M + [\Gamma, M] + \sigma(n \epsilon^\top) + \varrho_0\, \sigma(m\, b^\top R) + \Theta, \\ \Omega := R^\top \partial_t R,\ \Gamma := R^\top \partial_x R,\ \epsilon := R^\top \partial_x \phi. \end{cases} \tag{4.40}$$

From these, we get a characterization of the neutral configuration $(\phi = \phi_0, R = I_3)$, namely

$$\begin{cases} 0 = -g \varrho_0\, \mathrm{e_z} + \varrho_0 (\partial_\phi b)_{\phi_0}^\top\, m_{\phi_0} + f_{\phi_0, I_3}, \\ 0 = \varrho_0\, \sigma(m_{\phi_0}\, b_{\phi_0}^\top) + \Theta_{\phi_0, I_3}, \end{cases} \tag{4.41}$$

since an equilibrium configuration is characterized by the conditions $q = 0$, $\Pi = 0$, $n = 0$, $M = 0$, $\Omega = 0$, $\Gamma = 0$, and $\epsilon = \mathrm{e_x}$.

The key point is to express the actual configuration (ϕ, R) in terms of a small displacement in a geometrically sound way as

$$\begin{cases} R \approx I_3 + B, \\ \phi \approx \phi_0 + u, \end{cases} \tag{4.42}$$

where $B \in \mathfrak{so}(3)$ denotes a small-angle torsion (in every possible direction) and $u \in \mathbb{R}^3$ denotes a small displacement with respect to the neutral centerline and also characterized by a small spatial gradient $\partial_x u$. On the basis of these approximations, the following linearization is readily achieved:

$$\begin{cases} q \approx \varrho_0\, \partial_t u,\ \Omega \approx \partial_t B,\ \Gamma \approx \partial_x B, \\ \Pi \approx \sigma(J\, \partial_t B),\ M \approx \sigma(D\, \partial_x B),\ \epsilon \approx \partial_x u - \mathrm{e_x}, \\ n \approx C\, \partial_x u,\ b \approx b_{\phi_0} + (\partial_\phi b)_{\phi_0} u,\ \partial_\phi b \approx (\partial_\phi b)_{\phi_0} + (\partial_{\phi\phi} b)_{\phi_0} u, \\ f \approx f_{\phi_0, I_3} + (\partial_\phi f)_{\phi_0, I_3} u + (\partial_R f)_{\phi_0, I_3} B, \\ \Theta \approx \Theta_{\phi_0, I_3} + (\partial_\phi \Theta)_{\phi_0, I_3} u + (\partial_R \Theta)_{\phi_0, I_3} B, \end{cases} \tag{4.43}$$

where $(\partial_{\phi\phi} b)_{\phi_0} : \mathbb{R}^3 \to \mathbb{R}^{3\times 3}$, $(\partial_R f)_{\phi_0, I_3} : \mathfrak{so}(3) \to \mathbb{R}^3$, $(\partial_\phi \Theta)_{\phi_0, I_3} : \mathbb{R}^3 \to \mathfrak{so}(3)$ and $(\partial_R \Theta)_{\phi_0, I_3} : \mathfrak{so}(3) \to \mathfrak{so}(3)$.

On the basis of the expansions above, truncated to the first order, a breakdown of the terms that appear in the equations of motion (3.1) is derived as follows:

$$\begin{cases} \partial_t q \approx \varrho_0 \partial_{tt} u,\ \partial_x(R\,n) \approx \partial_x(C\,\partial_x u), \\ (\partial_\phi b)^\top R\,m \approx ((\partial_{\phi\phi} b)_{\phi_0} u)^\top m + (\partial_\phi b)^\top_{\phi_0}(m + B\,m), \\ \partial_t \Pi \approx \sigma(J\,\partial_{tt} B),\ [\Omega, \Pi] = -\sigma(J(\partial_t B)^2),\ \partial_x M \approx \partial_x \sigma(D \partial_x B), \\ [\Gamma, M] \approx -\sigma(D(\partial_x B)^2),\ \sigma(n\epsilon^\top) \approx \sigma(C \partial_x u \mathrm{e_x}^\top), \\ \sigma(m\,b^\top R) \approx \sigma(m\,b^\top_{\phi_0}(I_3 + B)) + \sigma(m\,u^\top(\partial_\phi b)^\top_{\phi_0}). \end{cases} \tag{4.44}$$

The resulting equations of motion, obtained by plugging the above expansion as well as the equilibrium conditions (4.41) into the exact relations (4.40), read as follows:

$$\begin{cases} \varrho_0\,\partial_{tt} u = \partial_x(C\,\partial_x u) + \varrho_0\,((\partial_{\phi\phi} b)_{\phi_0} u)^\top m + \varrho_0\,(\partial_\phi b)^\top_{\phi_0} B\,m \\ \qquad\qquad + (\partial_\phi f)_{\phi_0, I_3} u + (\partial_R f)_{\phi_0, I_3} B, \\ \partial_t \Pi - \sigma(J(\partial_t B)^2) = \partial_x \sigma(D \partial_x B) + \sigma(C\,\partial_x u\,\mathrm{e_x}^\top) + \varrho_0\,\sigma(m\,b^\top_{\phi_0} B) \\ \qquad\qquad + \varrho_0\,\sigma(m\,u^\top(\partial_\phi b)^\top_{\phi_0}) + (\partial_\phi \Theta)_{\phi_0, I_3} u + (\partial_R \Theta)_{\phi_0, I_3} B, \end{cases} \tag{4.45}$$

where we have neglected the term $\sigma(D(\partial_x B)^2)$ under the assumption that the spatial rate of twisting/tilting across the beam is moderate.

The linearized model (4.45) looks quite intricate because of the presence of external fields and solicitations. The equations of a free beam ($b \equiv 0$, $g \equiv 0$, $f \equiv 0$, $\Theta \equiv 0$) look much simpler:

$$\begin{cases} \varrho_0\,\partial_{tt} u = \partial_x(C\,\partial_x u), \\ \partial_t \Pi - \sigma(J(\partial_t B)^2) = \partial_x \sigma(D\,\partial_x B) + \sigma(C\,\partial_x u\,\mathrm{e_x}^\top). \end{cases} \tag{4.46}$$

Quite interestingly, under the same assumptions adopted in the linearization of the two-dimensional model, namely that the bending stiffness C is constant across the beam and that the cross-sectional inertia J is negligible, these two equations may be recast as

$$\begin{cases} \varrho_0\,\sigma(\partial_{tt} u\,\mathrm{e_x}^\top) = \sigma(C\,\partial_{xx} u \mathrm{e_x}^\top), \\ \sigma(C\,\partial_{xx} u\,\mathrm{e_x}^\top) = -\partial_{xx}\sigma(D\,\partial_x B). \end{cases} \tag{4.47}$$

In addition, interpreting the three independent components of the matrix B as small angles, it makes sense to introduce a geometric compatibility condition of the form

$$B = (\partial_x u)^\times, \tag{4.48}$$

where the symbol $(\star)^\times : \mathbb{R}^3 \to \mathfrak{so}(3)$ represents an operator (often referred to as a 'hat map' in geometric mechanics) that converts a vector into a skew-symmetric matrix. Combining this relation and the ones in (4.47) results in the equation in the displacement u:

$$\varrho_0\,\sigma(\partial_{tt} u\,\mathrm{e_x}^\top) + \partial_{xx}\sigma(D\,(\partial_{xx} u)^\times) = 0, \tag{4.49}$$

which represents a three-dimensional counterpart of the Euler-Bernoulli Eq (4.39). As usual, the stiffness matrix D incorporates some information about the geometric and mechanical properties of the beam, such as its Young's modulus, which may vary across a beam. If, however, this property is a constant of the beam, then the above equation simplifies to

$$\sigma(\varrho_0\,\partial_{tt} u\,\mathrm{e_x}^\top + D\,(\partial_{xxxx} u)^\times) = 0 \tag{4.50}$$

which remarkably appears as a three-dimensional version of the Euler-Bernoulli equation.

5. Conclusions

We have presented an account of geometrically exact beam theory using the framework of Lie groups, which offers a natural and robust description of large deformations and rotations in slender structures. By representing the beam configuration as a curve in the configuration space $\mathbb{SO}(3) \times \mathbb{R}^3$, the theory remains fully consistent with the underlying geometric structure of rigid body motions, avoiding the limitations of local coordinates or small-angle approximations.

The resulting equations of motion, derived from a variational principle, preserve essential physical quantities such as energy, linear momentum, and angular momentum under appropriate conditions. These conservation laws are fundamental from a physical standpoint and also play a key role in ensuring numerical stability when simulating beam's motion in space. The Lie group formulation naturally separates kinematics and dynamics: Measures of strain such as the axial/shear strains ϵ and Γ describe the beam deformation, while internal forces and moments are introduced via (linear) constitutive laws and evolve accordingly.

A distinctive feature of this approach is the appearance of Lie algebraic structures, such as the bracket $[\Gamma, M]$ in the angular momentum balance. These terms reflect intrinsic rotational interactions and are crucial to maintaining the correct coupling between motion and deformation. Proving the conservation of angular momentum within this setting can be subtle, often requiring integration by parts and leveraging algebraic identities related to skew-symmetric tensors.

Moreover, the Lie group formalism is compatible with structure-preserving numerical methods, such as discrete variational integrators. These methods respect the geometric nature of the physical system under analysis and ensure the exact conservation of both scalar and tensor-valued invariants, which is especially important for long-time dynamic simulations. The adopted approach also provides insights into the time evolution of the beam's centerline length and the consistency of the internal energy contributions.

Overall, the Lie group formulation of geometrically exact beam theory provides a powerful, physically consistent, and computationally advantageous framework for modeling slender structures undergoing large deformations.

Use of Generative-AI tools declaration

The authors declare that they have not used Artificial Intelligence (AI) tools in the creation of this article.

Acknowledgments

The author indebted to the anonymous reviewers, whose careful reading and insightful comments helped improve the presentation and content of the manuscript.

Conflict of interest

The author declares no conflict of interest.

References

1. K. G. Aktas, I. Esen, State-space modeling and active vibration control of smart flexible cantilever beam with the use of finite element method, *Eng. Technol. Appl. Sci. Res.*, **10** (2020), 6549–6556. https://doi.org/10.48084/etasr.3949
2. I. I. Andrianov, J. Awrejcewicz, W. T. van Horssen, On the Bolotin's reduced beam model versus various boundary conditions, *Mech. Res. Commun.*, **105** (2020), 103505. https://doi.org/10.1016/j.mechrescom.2020.103505
3. S. S. Antman, Nonlinear problems of elasticity, In: *Applied mathematical sciences*, 2 Eds., New York: Springer, 2005.
4. G. Aretusi, C. Cardillo, A. Salvatori, E. Bednarczyk, R. Fedele, A simple extension of Timoshenko beam model to describe dissipation in cementitious elements, *Zeitschrift Angewandte Math. Phys.*, **75** (2024), 166. https://doi.org/10.1007/s00033-024-02304-w
5. J. M. Aristoff, C. Clanet, J. W. Bush, The elastochrone: The descent time of a sphere on a flexible beam, *Proce. Royal Soc. A: Math. Phys. Eng. Sci.*, **465** (2009), 2293–2311. https://doi.org/10.1098/rspa.2009.0048
6. E. M. Bakr, A. A. Shabana, Application of Timoshenko beam theory to the dynamics of flexible legged locomotion, *J. Mech. Trans. Autom. Design*, **110** (1988), 28–34. https://doi.org/10.1115/1.3258900
7. S. Bali, Tukovi´c, P. Cardiff, A. Ivankovi´c, V. Pakrashi, A cell-centered finite volume formulation of geometrically exact simo–reissner beams with arbitrary initial curvatures, *Int. J. Numer. Meth. Eng.*, **123** (2022), 3950–3973. https://doi.org/10.1002/nme.6994
8. P. Betsch, *Structure-preserving integrators in nonlinear structural dynamics and flexible multibody dynamics*, Cham: Springer, 2016. https://doi.org/10.1007/978-3-319-31879-0
9. A. Bloch, J. Marsden, D. Zenkov, Nonholonomic dynamics, *Notices AMS*, **52** (2005), 320–329.
10. F. Boyer, G. De Nayer, A. Leroyer, M. Visonneau, Geometrically exact Kirchhoff beam theory: Application to cable dynamics, *J. Comput. Nonlinear Dyn.*, **6** (2011), 041004. https://doi.org/10.1115/1.4003625
11. G. Carcassi, C. Aidala, Geometric and physical interpretation of the action principle, *Sci. Rep.*, **13** (2023), 12138. https://doi.org/10.1038/s41598-023-39145-y
12. E. Cosserat, F. Cosserat, *Théorie des corps déformables*, Paris: Hermann et Fils, 1909.
13. O. Cosserat, L. L. Marrec, Timoshenko beam under finite and dynamic transformations: Lagrangian coordinates and Hamiltonian structures, preprint paper, 2025. https://doi.org/10.48550/arXiv.2407.14453
14. M. De Rosa, M. Lippiello, I. Elishakoff, Variational derivation of truncated Timoshenko- Ehrenfest beam theory, *J. Appl. Comput. Mech.*, **8** (2022), 996–1004. https://doi.org/10.22055/jacm.2022.39354.3394
15. F. Demoures, F. Gay-Balmaz, S. Leyendecker, S. Ober-Blöbaum, T. S. Ratiu, Y. Weinand, Discrete variational Lie group formulation of geometrically exact beam dynamics, *Numer. Math.*, **130** (2015), 73–123. https://doi.org/10.1007/s00211-014-0659-4

16. D. J. Dichmann, Y. Li, J. H. Maddocks, *Hamiltonian formulations and symmetries in rod mechanics*, New York: Springer, 1996. https://doi.org/10.1007/978-1-4612-4066-2_6

17. E. Dowell, K. McHugh, Equations of motion for an inextensible beam undergoing large deflections, *J. Appl. Mech.*, **83** (2016), 051007. https://doi.org/10.1115/1.4032795

18. H. Essén, A. Nordmark, A simple model for the falling cat problem, *European J. Phys.*, **39** (2018), 035004. https://doi.org/10.1088/1361-6404/aaac06

19. S. R. Eugster, J. Harsch, A variational formulation of classical nonlinear beam theories, In: *Developments and novel approaches in nonlinear solid body mechanics*, Cham: Springer International Publishing, 2020. https://doi.org/10.1007/978-3-030-50460-1_9

20. H. Farokhi, Y. Xia, A. Erturk, Experimentally validated geometrically exact model for extreme nonlinear motions of cantilevers, *Nonlinear Dyn.*, **105** (2021), 3005–3022. https://doi.org/10.1007/s11071-021-07023-9

21. S. Fiori, Coordinate-free Lie-group-based modeling and simulation of a submersible vehicle, *AIMS Math.*, **9** (2024), 10157–10184. https://doi.org/10.3934/math.2024497

22. S. Fiori, Lie-group modeling and simulation of a spherical robot, actuated by a yoke–pendulum system, rolling over a flat surface without slipping, *Robot. Auton. Syst.*, **175** (2024), 104660. https://doi.org/10.1016/j.robot.2024.104660

23. S. Fiori, L. Sabatini, F. Rachiglia, E. Sampaolesi, Modeling, simulation and control of a spacecraft: Automated reorientation under directional constraints, *Acta Astronaut.*, **216** (2024), 214–228. https://doi.org/10.1016/j.actaastro.2023.12.053

24. G. B. Folland, *Real analysis: Modern techniques and their applications*, 2 Eds., Hoboken: John Wiley & Sons, 1999.

25. C. Frohlich, The physics of somersaulting and twisting, *Sci. Amer.*, **242** (1980), 154–165. https://doi.org/10.1038/scientificamerican0380-154

26. J. Gerstmayr, M. K. Matikainen, A. M. Mikkola, A geometrically exact beam element based on the absolute nodal coordinate formulation, *Multibody Syst. Dyn.*, **20** (2008), 359–384. https://doi.org/10.1007/s11044-008-9125-3

27. S. Ghuku, K. N. Saha, A review on stress and deformation analysis of curved beams under large deflection, *Int. J. Eng. Technol.*, **11** (2017), 13–39. https://doi.org/10.56431/p-48538j

28. C. A. González-Cruz, J. C. Jauregui-Correa, G. Herrera-Ruiz, Nonlinear response of cantilever beams due to large geometric deformations: Experimental validation, *J. Mech. Eng.*, **62** (2016), 187–196. https://doi.org/10.5545/sv-jme.2015.2964

29. S. Gu, J. Chen, Q. Tian, An adaptive time-step energy-preserving variational integrator for flexible multibody system dynamics, *Appl. Math. Model.*, **138** (2025), 115759. https://doi.org/10.1016/j.apm.2024.115759

30. Z. V. Guo, L. Mahadevan, Limbless undulatory propulsion on land, *Proc. National Acad. Sci.*, **105** (2008), 3179–3184. https://doi.org/10.1073/pnas.0705442105

31. M. Herrmann, S. Leyendecker, Relative-kinematic formulation of geometrically exact beam dynamics based on Lie group variational integrators, *Comput. Meth. Appl. Mech. Eng.*, **432** (2024), 117375. https://doi.org/10.1016/j.cma.2024.117375

32. C. Howcroft, R. G. Cook, S. A. Neild, M. H. Lowenberg, J. E. Cooper, E. B. Coetzee, On the geometrically exact low-order modelling of a flexible beam: Formulation and numerical tests, *Proc. Royal Soc. A: Math. Phys. Eng. Sci.*, **474** (2018), 0423. https://doi.org/10.1098/rspa.2018.0423
33. K. Huang, X. Cai, M. Wang, Bernoulli-Euler beam theory of single-walled carbon nanotubes based on nonlinear stress-strain relationship, *Mater. Res. Express*, **7** (2020), 125003. https://doi.org/10.1088/2053-1591/abce86
34. G. Huber, D. Wollherr, M. Buss, A concise and geometrically exact planar beam model for arbitrarily large elastic deformation dynamics, *Front. Robot. AI*, **7** (2021), 609478. https://doi.org/10.3389/frobt.2020.609478
35. M. Javanmard, M. Bayat, A. Ardakani, Nonlinear vibration of Euler-Bernoulli beams resting on linear elastic foundation, *Steel Compos. Struct.*, **15** (2013), 439. https://doi.org/10.12989/scs.2013.15.4.439
36. G. Jelenic, M. Crisfield, Geometrically exact 3D beam theory: Implementation of a strain-invariant finite element for statics and dynamics, *Comput. Meth. Appl. Mech. Eng.*, **171** (1999), 141–171. https://doi.org/10.1016/S0045-7825(98)00249-7
37. P. Jung, S. Leyendeckery, J. Linnz, M. Ortiz, Discrete Lagrangian mechanics and geometrically exact Cosserat rods, In: *Multibody Dynamics 2009, ECCOMAS Thematic Conference, Warsaw, Poland,* 2009.
38. P. L. Kinon, P. Betsch, S. Schneider, Structure-preserving integrators based on a new variational principle for constrained mechanical systems, *Nonlinear Dyn.*, **111** (2023), 14231–14261. https://doi.org/10.1007/s11071-023-08542-4
39. S. K. Kota, S. Kumar, B. Giovanardi, A discontinuous Galerkin/cohesive zone model approach for the computational modeling of fracture in geometrically exact slender beams, *Comput. Mech.*, **75** (2025), 595–612. https://doi.org/10.1007/s00466-024-02521-0
40. H. Lang, J. Linn, M. Arnold, Multibody dynamics simulation of geometrically exact Cosserat rods, *Multibody Syst. Dyn.*, **25** (2011), 285–312. https://doi.org/10.1007/s11044-010-9223-x
41. T. Leitz, S. Ober-Blobaum, S. Leyendecker, Variational Lie group formulation of geometrically exact beam dynamics, In: *Synchronous and asynchronous integration*, Cham: Springer International Publishing, 175–203, 2014. https://doi.org/10.1007/978-3-319-07260-9_8
42. T. Leitz, R. T. Sato, M. de Almagro, S. Leyendecker, Multisymplectic Galerkin Lie group variational integrators for geometrically exact beam dynamics based on unit dual quaternion interpolation-no shear locking, *Comput. Meth. Appl. Mech. Eng.*, **374** (2021), 113475. https://doi.org/10.1016/j.cma.2020.113475
43. N. Lemos, Complete inequivalence of nonholonomic and vakonomic mechanics, *Acta Mech.*, **233** (2021), 47–56. https://doi.org/10.1007/s00707-021-03106-1
44. M. Levinson, A new rectangular beam theory, *J. Sound Vibr.*, **74** (1981), 81–87. https://doi.org/10.1016/0022-460X(81)90493-4
45. V. L. Litvinov, Variational formulation of the problem on vibrations of a beam with a moving spring-loaded support, *Theoret. Math. Phys.*, **215** (2023), 709–715. https://doi.org/10.1134/S0040577923050094

46. Y. Lu, X. Liu, H. Zhang, Dynamics of slender beam based on geometrically exact Kirchhoff beam theory formulated on SO(3) group, *Acta Mech. Sinica*, **40** (2024), 623017. https://doi.org/10.1007/s10409-023-23017-x

47. Z. Lu, Z. Zhang, Y. Yang, L. Dong, S. N. Atluri, Framework of physically consistent homogenization and multiscale modeling of beam structures, *AIAA J.*, **62** (2024), 4855–4869. https://doi.org/10.2514/1.J063902

48. C. Ma, M. Shao, J. Ma, C. Liu, K. Gao, Fluid structure interaction analysis of flexible beams vibrating in a time-varying fluid domain, *Proc. Inst. Mech. Eng. Part C*, **234** (2020), 1913–1927. https://doi.org/10.1177/0954406220902163

49. D. Manta, R. Gonçalves, A geometrically exact Kirchhoff beam model including torsion warping, *Comput. Struct.*, **177** (2016), 192–203. https://doi.org/10.1016/j.compstruc.2016.08.013

50. T. McDonnell, A. Ning, Geometrically exact beam theory for gradient-based optimization, *Comput. Struct.*, **298** (2024), 107373. https://doi.org/10.1016/j.compstruc.2024.107373

51. C. Meier, A. Popp, W. Wall, Geometrically exact finite element formulations for slender beams: Kirchhoff–Love theory versus Simo-Reissner theory, *Arch. Comput. Meth. Eng.*, **26** (2019), 163–243. https://doi.org/10.1007/s11831-017-9232-5

52. J. Nabeshima, M. H. D. Y. Saraiji, K. Minamizawa, Arque: Artificial biomimicry-inspired tail for extending innate body functions, In: *ACM SIGGRAPH 2019 Posters, SIGGRAPH '19*, 2019, 52. https://doi.org/10.1145/3306214.3338573

53. R. Nzengwa, Lagrange multiplier and variational equations in mechanics, *J. Eng. Math.*, **144** (2024), 5. https://doi.org/10.1007/s10665-023-10299-y

54. P. F. Pai, Geometrically exact beam theory without Euler angles, *Int. J. Solids Struct.*, **48** (2011), 3075–3090. https://doi.org/10.1016/j.ijsolstr.2011.07.003

55. N. Peres, R. Gonçalves, D. Camotim, A geometrically exact beam finite element for curved thin-walled bars with deformable cross-section, *Comput. Meth. Appl. Mech. Eng.*, **381** (2021), 113804. https://doi.org/10.1016/j.cma.2021.113804

56. J. N. Reddy, *Mechanics of laminated composite plates and shells: Theory and analysis*, Boca Raton: CRC Press, 1993.

57. L. Reti, *The unknown Leonardo*, New York: McGraw-Hill, 1974.

58. C. Rodriguez, Networks of geometrically exact beams: Well-posedness and stabilization, *Math. Control Related Fields*, **12** (2022), 49–80. https://doi.org/10.3934/mcrf.2021002

59. C. Rodriguez, G. Leugering, Boundary feedback stabilization for the intrinsic geometrically exact beam model, *SIAM J. Control Optim.*, **58** (2020), 3533–3558. https://doi.org/10.1137/20M1340010

60. M. Shao, C. Ma, S. Hu, C. Sun, D. Jing, Effects of time-varying fluid on dynamical characteristics of cantilever beams: Numerical simulations and experimental measurements, *Math. Probl. Eng.*, **2020** (2020), 6679443. https://doi.org/10.1155/2020/6679443

61. R. W. Sharpe, *Differential geometry: Cartan's generalization of Klein's erlangen program*, New York: Springer, 1997. https://doi.org/10.1007/978-1-4612-0691-2

62. J. Simo, L. Vu-Quoc, A three-dimensional finite-strain rod model. Part II: Computational aspects, *Comput. Meth. Appl. Mech. Eng.*, **58** (1986), 79–116. https://doi.org/10.1016/0045-7825(86)90079-4

63. N. Singh, I. Sharma, S. S. Gupta, Dynamics of variable length geometrically exact beams in three-dimensions, *Int. J. Solids Struct.*, **191-192** (2020), 614–627. https://doi.org/10.1016/j.ijsolstr.2019.11.005

64. V. Sonneville, A. Cardona, O. Brüls, Geometrically exact beam finite element formulated on the special Euclidean group SE(3), *Comput. Meth. Appl. Mech. Eng.*, **268** (2014), 451–474. https://doi.org/10.1016/j.cma.2013.10.008

65. A. Tariverdi, V. K. Venkiteswaran, Ø. G. Martinsen, O. J. Elle, J. Tørresen, S. Misra, Dynamic modeling of soft continuum manipulators using Lie group variational integration, *PLoS One*, **15** (2020), e0236121. https://doi.org/10.1371/journal.pone.0236121

66. S. P. Timoshenko, J. M. Gere, *Strength of materials, Part 1: Elementary theory and problems*, 2 Eds., New York: Van Nostrand, 1955.

67. V. Tojaga, T. C. Gasser, A. Kulachenko, S. Östlund, A. Ibrahimbegovic, Geometrically exact beam theory with embedded strong discontinuities for the modeling of failure in structures. Part I: Formulation and finite element implementation, *Comput. Meth. Appl. Mech. Eng.*, **410** (2023), 116013. https://doi.org/10.1016/j.cma.2023.116013

68. A. P. Tzes, S. Yurkovich, F. D. Langer, A method for solution of the Euler-Bernoulli beam equation in flexible-link robotic systems, In: *IEEE 1989 International Conference on Systems Engineering*, 1989, 557–560. https://doi.org/10.1109/ICSYSE.1989.48736

69. K. Wu, G. Zheng, A comprehensive static modeling methodology via beam theory for compliant mechanisms, *Mech. Mach. Theory*, **169** (2022), 104598. https://doi.org/10.1016/j.mechmachtheory.2021.104598

70. Q. Wu, N. Zhao, M. Yao, Y. Niu, C. Wang, Free vibrations and frequency sensitivity of bionic microcantilevers with stress concentration effect, *Int. J. Struct. Stability Dyn.*, 2025. https://doi.org/10.1142/S0219455426502226

71. W. S. Yoo, J. H. Lee, S. J. Park, J. H. Sohn, O. Dmitrochenko, D. Y. Pogorelov, Large oscillations of a thin cantilever beam: Physical experiments and simulation using the absolute nodal coordinate formulation, *Nonlinear Dyn.*, **34** (2003), 3–29. https://doi.org/10.1023/B:NODY.0000014550.30874.cc

AIMS Press